

See discussions, stats, and author profiles for this publication at: <https://www.researchgate.net/publication/343252791>

Conservative semi-Lagrangian schemes for kinetic equations Part I: Reconstruction

Preprint · July 2020

CITATIONS
0

READS
48

4 authors, including:



Sebastiano Boscarino
University of Catania
41 PUBLICATIONS 678 CITATIONS

[SEE PROFILE](#)



Giovanni Russo
University of Catania
267 PUBLICATIONS 6,298 CITATIONS

[SEE PROFILE](#)



Seok-Bae Yun
Sungkyunkwan University
69 PUBLICATIONS 520 CITATIONS

[SEE PROFILE](#)

Some of the authors of this publication are also working on these related projects:



Multiscale methods for hyperbolic and kinetic equations in diffusive regimes [View project](#)



Numerical methods for PDEs on Cartesian meshes for moving boundaries [View project](#)

CONSERVATIVE SEMI-LAGRANGIAN SCHEMES FOR KINETIC EQUATIONS

PART I: RECONSTRUCTION

SEUNG YEON CHO, SEBASTIANO BOSCARINO, GIOVANNI RUSSO, AND SEOK-BAE YUN

ABSTRACT. In this paper, we propose and analyse a reconstruction technique which enables one to design high-order conservative semi-Lagrangian schemes for kinetic equations. The proposed reconstruction can be obtained by taking the sliding average of a given polynomial reconstruction of the numerical solution. A compact representation of the high order conservative reconstruction in one and two space dimension is provided, and its mathematical properties are analyzed. To demonstrate the performance of proposed technique, we consider implicit semi-Lagrangian schemes for kinetic-like equations such as the Xin-Jin model and the Broadwell model, and then solve related shock problems which arise in the relaxation limit. Applications to BGK and Vlasov-Poisson equations will be presented in the second part of the paper.

1. INTRODUCTION

Kinetic equations and quasi-linear systems of conservation laws are strongly related. For example, the behavior of rarefied gas is well described by the Boltzmann transport equation (BTE) [10]. Once velocity space is discretized, BTE has the mathematical structure of a semi-linear hyperbolic system of balance laws. In the so-called fluid dynamic limit, the distribution function approaches the Maxwellian whose parameters satisfy the Euler equations of gas dynamics, which is a quasi-linear system of conservation laws. The Broadwell model of the BTE in one space dimension is a semi-linear 3×3 relaxation system. As the relaxation parameter vanishes, the model relaxes to a 2×2 quasi-linear hyperbolic system of conservation laws. An implicit treatment of the collision term using L-stable schemes allows the construction of asymptotic preserving schemes which become consistent schemes of the relaxed limit [4, 22, 31].

Quasi-linear hyperbolic systems generically develop jump discontinuities in finite time. Most schemes for their numerical solutions are based on two fundamental ingredients: conservation and non-oscillatory reconstruction. Finite volume and finite difference methods have been widely used for the discretization of the convective terms of kinetic models (Eulerian approach), which are usually treated explicitly. In this way, it is relatively easy to construct conservative schemes. Conservation is relevant especially in the relaxed limit: lack of conservation will prevent weak consistency of the method for discontinuous solutions leading, for example, to $\mathcal{O}(1)$ errors in the propagation of shocks.

Conservative non-oscillatory reconstruction such as the ENO or WENO methodology [35] have been widely adopted in many practical problems [7, 9, 30]. The approach has been extended to a compact WENO (CWENO [6, 12, 13, 27–29]) reconstruction which gives uniform accuracy in a whole cell, and it allows the construction of efficient high order finite volume scheme in several space dimensions [16]. Unfortunately, explicit Eulerian schemes cannot avoid CFL-type time step restrictions imposed by convection-like terms in hyperbolic equations.

To treat this difficulty, semi-Lagrangian approaches recently have gained popularity because they do not suffer from such CFL-type time step restriction which arises in the treatment of Eulerian counterparts. Instead, since the semi-Lagrangian method is obtained by integrating the equations along its characteristics, this approach necessarily requires the computation of numerical solutions on off-grid points by a reconstruction which makes use of the numerical solutions on grid points.

If one uses piecewise Lagrange polynomial reconstruction, then conservation is guaranteed if the same stencil is used in each cell, because of translation invariance (we shall call this a *linear reconstruction*). On the other hand, such linear reconstruction may introduce spurious oscillations of may

cause loss of positivity. If one wants to prevent appearing of spurious oscillations, then one can use high-order non-oscillatory reconstruction, such as ENO or WENO [7, 8, 35]. Similarly, positivity of the numerical solution can be maintained by positivity-preserving reconstructions [5, 34]. Unfortunately these non-linear reconstructions destroy the translation invariance guaranteed by linear reconstruction, causing lack of conservation [1].

Numerous approaches have been introduced to treat such difficulties, and maintain conservation even with non-linear reconstruction. In particular, in the context of Vlasov-Poisson system several techniques were proposed. Among them, we mention the work based on primitive polynomial reconstruction [14, 18, 32]. In [18], the authors developed the Positive and Flux Conservative scheme. The authors considered essentially non-oscillatory method (ENO) or reconstructions based on positive limiters. In [14], the authors took a similar approach in the construction of primitive functions using splines. An weighted essentially non-oscillatory method (WENO) is also proposed to construct high order conservative non-oscillatory schemes in [32]. All these method are either one-dimensional or they provide a dimension by dimension interpolation. A general technique to restore conservation in semi-Lagrangian schemes was presented in [33]. The technique has been also applied to the BGK model [1]. Although quite general, the technique suffers from CFL-type stability restrictions.

In this paper we present a general technique which allows the construction of high-order conservative non-oscillatory semi-Lagrangian schemes in one and several dimensions, which are not affected by CFL-type restriction. Given cell averaged values on uniform grids, the idea is to compute sliding average of a precomputed non-oscillatory piecewise polynomial reconstruction.

The resulting reconstruction inherits the non-oscillatory properties of the precomputed polynomial and guarantees conservation of all discrete moments. The technique requires characteristic lines are parallel, which is the case of kinetic equations in which velocity space is discretized on the same velocity grid throughout space. An advantage of our method is that one can easily adopt previous techniques such as ENO, WENO, CWENO polynomials as our basic reconstructions.

The mathematical properties of the proposed reconstruction are analyzed. In particular, we show that if we take CWENO polynomials of even degree k , for example $k = 2, 4$ [6, 28], as a basic reconstruction, our approach gives $k + 2$ th order accuracy. Similar properties are also generalized to two dimensional reconstruction with CWENO polynomial in two space dimensions [28]. The description of technique is provided in the sense of cell averages, however, the idea can be extended to the point-wise framework in a similar manner.

To test the quality of the proposed reconstruction, we apply it to the finite difference implicit semi-Lagrangian schemes for semi-linear hyperbolic system such as Xin-Jin model or Broadwell model. Applications to more general equations will be presented in a companion paper.

This paper is organized as follows: In section 2, we present a general framework for our conservative reconstruction in 1D and its related properties. section 3 is devoted to the conserative reconstruction in 2D. Semi-Lagrangian methods are described in section 4. In section 5, several numerical tests are presented to verify the accuracy of the proposed schemes and its capability in treating shocks arising in the relaxation of semi-linear hyperbolic system.

2. CONSERVATIVE RECONSTRUCTION IN 1D

Let $u : \mathbb{R} \rightarrow \mathbb{R}$ be a smooth function and $\bar{u} : \mathbb{R} \rightarrow \mathbb{R}$ be a corresponding sliding average function:

$$\frac{1}{\Delta x} \int_{x-\Delta x/2}^{x+\Delta x/2} u(y) dy = \bar{u}(x).$$

Given cell averages on uniform grids $x_i = i\Delta x$:

$$\frac{1}{\Delta x} \int_{I_i} u(x) dx = \bar{u}_i, \quad I_i = [x_{i-\frac{1}{2}}, x_{i+\frac{1}{2}}],$$

for each $i \in \mathcal{I}$, our goal is to construct an approximation $Q(x)$ of the sliding average $\bar{u}(x)$, which is conservative in the sense that for any periodic function $\bar{u}(x)$ with period $L = N\Delta x$, $N \in \mathbb{N}$, we have

$$\sum_{i=1}^N Q(x_i + \theta) = \sum_{i=1}^N \bar{u}(x_i), \quad \theta \in [0, 1].$$

Assume we have a piecewise smooth reconstruction $R(x) = \sum_i R_i(x)\chi_i(x)$, for $i \in \mathcal{I}$, where $\chi_i(x)$ denotes the characteristic function of cell i and each $R_i(x)$ denotes a polynomial of degree k and has the following properties:

- (1) High order accuracy in the approximation of $u(x)$:

$$(2.1) \quad u(x) = R_i(x) + \mathcal{O}((\Delta x)^{k+1}), \quad x \in I_i.$$

- (2) Conservation in the sense of cell averages:

$$\frac{1}{\Delta x} \int_{x_{i-\frac{1}{2}}}^{x_{i+\frac{1}{2}}} R_i(x) dx = \bar{u}_i.$$

Consider a shifted interval $[y_{i-\frac{1}{2}}, y_{i+\frac{1}{2}}]$ whose center is $x_{i+\theta} \equiv x_i + \theta\Delta x$, $\theta \in [0, 1]$, and denote by $\bar{u}(x_{i+\theta})$ the sliding average of u at $x_{i+\theta}$ (see Fig. 1). We see that

$$x_{i-\frac{1}{2}} \leq y_{i-\frac{1}{2}} < x_{i+\frac{1}{2}} \leq y_{i+\frac{1}{2}} < x_{i+\frac{3}{2}}.$$

Our strategy is to approximate $\bar{u}(x_{i+\theta})$ by $Q_{i+\theta} \equiv Q(x_{i+\theta})$, where

$$(2.2) \quad Q_{i+\theta} = \frac{1}{\Delta x} \int_{y_{i-\frac{1}{2}}}^{y_{i+\frac{1}{2}}} R(x) dx = \frac{1}{\Delta x} \int_{x_{i-\frac{1}{2}+\theta}}^{x_{i+\frac{1}{2}+\theta}} R(x) dx,$$

which is equivalent to

$$(2.3) \quad Q_{i+\theta} = \frac{1}{\Delta x} \int_{x_{i-\frac{1}{2}+\theta}}^{x_{i+\frac{1}{2}}} R_i(x) dx + \frac{1}{\Delta x} \int_{x_{i+\frac{1}{2}}}^{x_{i+\frac{1}{2}+\theta}} R_{i+1}(x) dx.$$

From now on, we consider $R_i(x)$ to be piecewise polynomials of degree k of the form:

$$(2.4) \quad R_i(x) = \sum_{\ell=0}^k \frac{R_i^{(\ell)}}{\ell!} (x - x_i)^\ell.$$

Making use of (2.4) in the first term, we obtain

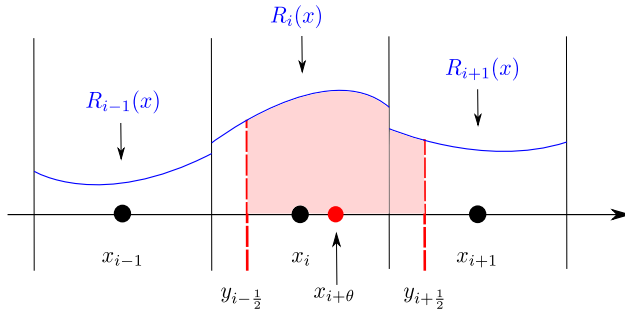


FIGURE 1. Description of one-dimensional conservative reconstruction

$$\frac{1}{\Delta x} \int_{x_{i-\frac{1}{2}+\theta}}^{x_{i+\frac{1}{2}}} R_i(x) dx = \frac{1}{\Delta x} \sum_{\ell=0}^k R_i^{(\ell)} \int_{x_{i-\frac{1}{2}+\theta}}^{x_{i+\frac{1}{2}}} \frac{1}{\ell!} (x - x_i)^\ell dx = \sum_{\ell=0}^k (\Delta x)^\ell R_i^{(\ell)} \alpha_\ell(\theta)$$

where

$$(2.5) \quad \alpha_\ell(\theta) = \frac{1 - (2\theta - 1)^{\ell+1}}{2^{\ell+1}(\ell + 1)!}.$$

Similarly, we can write

$$\frac{1}{\Delta x} \int_{x_{i+\frac{1}{2}}}^{x_{i+\frac{1}{2}+\theta}} R_{i+1}(x) dx := \sum_{\ell=0}^k (\Delta x)^\ell R_{i+1}^{(\ell)} \beta_\ell(\theta),$$

with

$$(2.6) \quad \beta_\ell(\theta) = \frac{(2\theta - 1)^{\ell+1} - (-1)^{\ell+1}}{2^{\ell+1}(\ell + 1)!}.$$

Letting $Q_{i+\theta}$ denote the approximation of $\bar{u}(x_{i+\theta})$, we obtain

$$(2.7) \quad Q_{i+\theta} := \sum_{\ell=0}^k (\Delta x)^\ell \left(\alpha_\ell(\theta) R_i^{(\ell)} + \beta_\ell(\theta) R_{i+1}^{(\ell)} \right).$$

Here, we note that $\alpha_\ell(\theta)$ and $\beta_\ell(\theta)$ satisfy the following relations:

- If $\ell = 2n$, $0 \leq n$, is an even number

$$(2.8) \quad \alpha_\ell(\theta) + \beta_\ell(\theta) = \frac{1}{(2n+1)!} \left(\frac{1}{2} \right)^{2n}.$$

- If $\ell = 2n+1$, $0 \leq n$, is an odd number

$$(2.9) \quad \alpha_\ell(\theta) + \beta_\ell(\theta) = 0.$$

We list the explicit form of $\alpha_\ell(\theta)$ and $\beta_\ell(\theta)$ for $\ell = 0, 1, 2$:

$$(2.10) \quad \begin{aligned} \alpha_0(\theta) &= 1 - \theta, & \alpha_1(\theta) &= \frac{\theta(1-\theta)}{2}, & \alpha_2(\theta) &= \frac{1-q(\theta)}{24} \\ \beta_0(\theta) &= \theta, & \beta_1(\theta) &= -\frac{\theta(1-\theta)}{2}, & \beta_2(\theta) &= \frac{q(\theta)}{24}, \end{aligned}$$

where $q(\theta) = 3\theta - 6\theta^2 + 4\theta^3$, for $\theta \in [0, 1]$.

2.1. General Properties. In this section, we provide several properties of the reconstruction (2.7) such as accuracy, conservation and consistency to the classical interpolation with a suitable choice of $R_i^{(\ell)}$ in the reconstruction.

Recalling the assumption (2.1), we have a function $R(x)$ which approximates point values of u and our goal is to approximate sliding average function \bar{u} with our reconstruction (2.7). Before checking the accuracy order, we note that the cell average function $\bar{u}(x)$ can be expressed in terms of derivatives of function $u(x)$:

$$(2.11) \quad \bar{u}(x) = \frac{1}{\Delta x} \int_{x-\Delta x/2}^{x+\Delta x/2} u(y) dy = \frac{1}{\Delta x} \int_{x-\Delta x/2}^{x+\Delta x/2} \sum_{\ell=0}^{\infty} \frac{u^{(\ell)}(x)}{\ell!} (y-x)^\ell dy = \sum_{\ell=\text{even}}^{\infty} (\Delta x)^\ell u^{(\ell)}(x) \frac{1}{(\ell+1)!} \left(\frac{1}{2} \right)^\ell.$$

Inserting $x = x_{i+\theta}$ into (2.11), we obtain

$$\bar{u}(x_{i+\theta}) = \sum_{\ell=\text{even}}^{\infty} (\Delta x)^\ell u^{(\ell)}(x_{i+\theta}) \frac{1}{(\ell+1)!} \left(\frac{1}{2} \right)^\ell = u^{(0)}(x_{i+\theta}) + \frac{(\Delta x)^2}{24} u^{(2)}(x_{i+\theta}) + \frac{(\Delta x)^4}{1920} u^{(4)}(x_{i+\theta}) + \dots$$

With this formula, in the following proposition, we provide a sufficient condition for a polynomial reconstruction $Q_{i+\theta}$ to be a $(k+2)$ -th order accurate approximation of $\bar{u}(x+\theta)$ for $\theta \in [0, 1]$.

Proposition 2.1. Let $k \geq 0$ be an even integer, $R_i \in \mathbb{P}^k$ be given by (2.4), and u be a smooth function $u : \mathbb{R} \rightarrow \mathbb{R}$. Suppose we have a piecewise polynomial $R(x) = \sum_i R_i(x) \chi_i(x)$, which satisfies

$$(2.12) \quad \begin{aligned} u_i^{(\ell)} &= R_i^{(\ell)} + \mathcal{O}(\Delta x^{k+2-\ell}), \quad 0 \leq \ell \leq k, \text{ whenever } \ell \text{ is an even integer} \\ u_i^{(\ell)} - u_{i+1}^{(\ell)} &= R_i^{(\ell)} - R_{i+1}^{(\ell)} + \mathcal{O}(\Delta x^{k+2-\ell}), \quad 0 \leq \ell < k, \text{ whenever } \ell \text{ is an odd integer.} \end{aligned}$$

Then, the reconstruction $Q_{i+\theta}$ gives a $(k+2)$ -th order approximation of the sliding average $\bar{u}(x_{i+\theta})$ for any $\theta \in [0, 1)$.

Proof. For detailed proof, see A. \square

Remark 2.1. (1) The reconstruction $Q_{i+\theta}$ approximates $\bar{u}(x_{i+\theta})$ on the basis of cell average values $\{\bar{u}_i\}_{i \in \mathcal{I}}$. Similarly, we can extend the idea of reconstruction to the framework of point values, which are used in conservative finite difference methods in section 4.
(2) We also note that the second condition in (2.12) can be easily satisfied. Let $k \geq 0$ be an even integer, and consider a function $u(x) \in C^{k+2}(\mathbb{R})$, and its primitive function $U(x) := \int_{-\infty}^x u(y) dy \in C^{k+3}(\mathbb{R})$. We first look for a polynomial $P_i(x) \in \mathbb{P}^{k+1}$ such that

$$P_i(x_{i-\frac{1}{2}+j}) = U(x_{i-\frac{1}{2}+j}), \quad j = -r, \dots, s+1, \quad r+s = k.$$

Then, the classical interpolation theory gives

$$U(x) - P_i(x) = \frac{1}{(k+2)!} U^{(k+2)}(\xi_i) \prod_{j=-r}^{s+1} (x - x_{i-\frac{1}{2}+j}), \quad \xi_i \in (x_{i-\frac{1}{2}-r}, x_{i+\frac{1}{2}+s}),$$

its first order derivative $p_i(x) \equiv P'_i(x) \in \mathbb{P}^k$ interpolates u in the sense of cell-average:

$$\frac{1}{\Delta x} \int_{x_{i+j}-\Delta x/2}^{x_{i+j}+\Delta x/2} p_i(y) dy = \bar{u}_{i+j}, \quad j = -r, \dots, s,$$

and, for $0 \leq \ell \leq k$, its $(\ell+1)$ -th derivative $p_i^{(\ell)}(x) \equiv P_i^{(\ell+1)}(x) \in \mathbb{P}^{k-\ell}$ satisfies

$$(2.13) \quad u^{(\ell)}(x) - p_i^{(\ell)}(x) = U^{(\ell+1)}(x) - P_i^{(\ell+1)}(x) = \frac{1}{(k+2)!} U^{(k+2)}(\xi_i) \frac{d^{\ell+1}}{dx^{\ell+1}} \left(\prod_{j=-r}^{s+1} (x - x_{i-\frac{1}{2}+j}) \right).$$

Similarly, we can find polynomials $p_{i+1}(x) \in \mathbb{P}^k$ and $P_{i+1}(x) \in \mathbb{P}^{k+1}$ such that

$$\begin{aligned} u^{(\ell)}(x + \Delta x) - p_{i+1}^{(\ell)}(x + \Delta x) &= U^{(\ell+1)}(x + \Delta x) - P_{i+1}^{(\ell+1)}(x + \Delta x) \\ &= \frac{1}{(k+2)!} U^{(k+2)}(\xi_{i+1}) \frac{d^{\ell+1}}{dx^{\ell+1}} \left(\prod_{j=-r}^{s+1} (x + \Delta x - x_{i+1-\frac{1}{2}+j}) \right), \end{aligned}$$

where $\xi_{i+1} \in (x_{i+\frac{1}{2}-r}, x_{i+\frac{3}{2}+s})$. Then, the relation $U^{(k+2)}(\xi_i) - U^{(k+2)}(\xi_{i+1}) = \mathcal{O}(\Delta x)$, gives

$$\begin{aligned} &\left(u^{(\ell)}(x_i) - p_i^{(\ell)}(x_i) \right) - \left(u^{(\ell)}(x_{i+1}) - p_{i+1}^{(\ell)}(x_{i+1}) \right) \\ &= \frac{1}{(k+2)!} \left(U^{(k+2)}(\xi_i) - U^{(k+2)}(\xi_{i+1}) \right) \left\{ \frac{d^\ell}{dx^\ell} \left(\prod_{j=-r}^{s+1} (x - x_{i-\frac{1}{2}+j}) \right) \right\}_{x=x_i} = \mathcal{O}((\Delta x)^{k+2-\ell}). \end{aligned}$$

(3) If $R_i^{(\ell)}$ can be represented with a Lipschitz function F_ℓ :

$$R_i^{(\ell)} = F_\ell(\bar{u}_{i-r}, \dots, \bar{u}_{i+s})$$

which satisfies

$$F_\ell(\bar{u}_{i-r}, \dots, \bar{u}_{i+s}) - u^{(\ell)}(x_i) = \mathcal{O}((\Delta x)^{k+1-\ell}),$$

the condition (2.12) is also satisfied. For more details, we refer to B.

In Proposition 2.1, we see that the choice of an even integer $k \geq 0$ leads to the improvement of accuracy. In such a case, we show that the reconstruction $Q_{i+\theta}$ based on linear weights coincides with the classical interpolation.

Proposition 2.2. *Let $k \geq 0$ be an even integer with $k = 2r$. For each $i \in \mathcal{I}$, assume that we have a basic reconstruction $R_i(x) \in \mathbb{P}^k$, which is a polynomial of degree k in (2.4) and interpolates the function u in the sense of cell averages:*

$$(2.14) \quad \frac{1}{\Delta x} \int_{x_{i+j-\frac{1}{2}}}^{x_{i+j+\frac{1}{2}}} R_i(x) dx = \bar{u}_{i+j}, \quad -r \leq j \leq r.$$

with a symmetric stencil $S_i := \{i-r, i-r+1, \dots, i+r\}$. Then, the reconstruction $Q_{i+\theta}$ in (2.7) based on R_i and R_{i+1} , is the Lagrange polynomial $L(x)$ that interpolates \bar{u}_{i+j} , for $-r \leq j \leq r+1$, where $x = x_i + \theta \Delta x$ and $\theta \in [0, 1]$.

The proof is based on the observation that interpolation in the sense of the cell averages is equivalent to point-wise interpolation of sliding averages at cell center, which in turn, is equivalent to point-wise interpolation of primitive function at cell edges. A detailed proof, based on explicit representation obtained by Lagrange interpolation, is given in C.

Remark 2.2. For $k = 0$, the only possible choice is to set $R_i(x) \equiv \bar{u}_i$ and the resulting reconstruction $Q_{i+\theta}$ reduces to the linear interpolation constructed from two points \bar{u}_i and \bar{u}_{i+1} .

In the following proposition, we show that total mass is preserved for any θ -shifted summation, $\theta \in [0, 1]$.

Proposition 2.3. *Assume that $R_i(x)$ satisfies*

$$(2.15) \quad \frac{1}{\Delta x} \int_{x_{i-\frac{1}{2}}}^{x_{i+\frac{1}{2}}} R_i(x) dx = \bar{u}_i, \quad i \in \mathcal{I}.$$

Then, for periodic functions $\bar{u}(x)$ with period $L = N \Delta x$, $N \in \mathbb{N}$

$$(2.16) \quad \sum_{i=1}^N Q_{i+\theta} = \sum_{i=1}^N \bar{u}_i,$$

for any $\theta \in [0, 1)$.

Proof. Since θ does not depend on i ,

$$\begin{aligned} \sum_{i=1}^N Q_{i+\theta} &= \sum_{i=1}^N \left(\frac{1}{\Delta x} \int_{x_{i-\frac{1}{2}}+\theta}^{x_{i+\frac{1}{2}}} R_i(x) dx + \frac{1}{\Delta x} \int_{x_{i+\frac{1}{2}}}^{x_{i+\frac{1}{2}}+\theta} R_{i+1}(x) dx \right) \\ &= \sum_{i=1}^N \left(\frac{1}{\Delta x} \int_{x_{i-\frac{1}{2}}+\theta}^{x_{i+\frac{1}{2}}} R_i(x) dx + \frac{1}{\Delta x} \int_{x_{i-\frac{1}{2}}}^{x_{i-\frac{1}{2}}+\theta} R_i(x) dx \right) \\ &= \sum_{i=1}^N \frac{1}{\Delta x} \int_{x_{i-\frac{1}{2}}}^{x_{i+\frac{1}{2}}} R_i(x) dx = \sum_{i=1}^N \bar{u}_i. \end{aligned}$$

Here we used the periodicity to write the second line and (2.15) for the last line. \square

Remark 2.3. We remark that this summation preserving property can be useful when our reconstruction is applied to the semi-Lagrangian treatment of a constant convection term, where characteristic curves are given by parallel lines for each grid point. In such cases, the proposed reconstruction attains conservation at a discrete level, hence it can be applied to the simulation of physical models satisfying this conservation property. Considerable examples are the BGK type models of the Boltzmann equation of rarefied gas dynamics. We can also apply this to the splitting method for the Vlasov-Poisson system in plasma physics. These problems will be considered in the second part of this paper.

In the following section, we will show that our reconstruction (2.7) inherits some properties of the basic reconstruction $R_i(x)$ such as non-oscillatory property and positivity.

2.2. Choice of the basic reconstruction R .

2.2.1. Non-oscillatory property. We consider some specific choices of the basic reconstruction R . In particular, we consider CWENO [6], [28] and CWENOZ [13]. As an illustration, we consider the case $k = 2$, and we take CWENO23 reconstruction in [28] as a basic reconstruction R . We start from a polynomial of degree two $P_{OPT}^i(x)$ which interpolates $\bar{u}_{i-1}, \bar{u}_i, \bar{u}_{i+1}$ in the sense of cell averages:

$$\frac{1}{\Delta x} \int_{x_{i+l-\frac{1}{2}}}^{x_{i+l+\frac{1}{2}}} P_{OPT}^i(x) dx = \bar{u}_{i+l}, \quad l = -1, 0, 1.$$

Then, this polynomial can be written as $P_{OPT}^i(x) = \tilde{u}_i + \tilde{u}'_i(x - x_i) + \frac{1}{2}\tilde{u}''_i(x - x_i)^2$ with

$$\tilde{u}_i = \bar{u}_i - \frac{1}{24}(\bar{u}_{i+1} - 2\bar{u}_i + \bar{u}_{i-1}), \quad \tilde{u}'_i = \frac{\bar{u}_{i+1} - \bar{u}_{i-1}}{2\Delta x}, \quad \tilde{u}''_i = \frac{\bar{u}_{i+1} - 2\bar{u}_i + \bar{u}_{i-1}}{(\Delta x)^2},$$

and it gives a third order accurate reconstruction of u in I_i :

$$P_{OPT}^i(x) = u(x) + \mathcal{O}(\Delta x)^3, \quad \forall x \in I_i.$$

In the CWENO23 reconstruction, to avoid oscillations, we use the following convex combination:

$$(2.17) \quad R_i(x) = \sum_k \omega_k^i P_k^i(x), \quad \sum_k \omega_k^i = 1, \quad \omega_k^i \geq 0, \quad k \in \{L, C, R\}$$

where P_L^i and P_R^i are first order polynomials such that

$$\int_{x_{i+l-\frac{1}{2}}}^{x_{i+l+\frac{1}{2}}} P_L^i(x) dx = \bar{u}_{i+l}, \quad l = -1, 0, \quad \int_{x_{i+l-\frac{1}{2}}}^{x_{i+l+\frac{1}{2}}} P_R^i(x) dx = \bar{u}_{i+l}, \quad l = 0, 1,$$

which gives

$$P_L^i(x) = \bar{u}_i + \frac{\bar{u}_i - \bar{u}_{i-1}}{\Delta x}(x - x_i), \quad P_R^i(x) = \bar{u}_i + \frac{\bar{u}_{i+1} - \bar{u}_i}{\Delta x}(x - x_i).$$

The second order polynomial $P_C(x)$ is obtained from

$$P_{OPT}^i(x) = C_L P_L^i(x) + C_R P_R^i(x) + C_C P_C^i(x),$$

with a choice of positive coefficients such that

$$C_L, C_R, C_C \geq 0, \quad C_L = C_R, \quad C_L + C_C + C_R = 1.$$

A common choice is to set $C_L = C_R = 1/4$, $C_C = 1/2$. The non-linear weights ω_k^i in (2.17) are chosen as follows:

$$(2.18) \quad \omega_k^i = \frac{\alpha_k^i}{\sum_\ell \alpha_\ell^i}, \quad \alpha_k^i = \frac{C_i}{(\epsilon + \beta_k^i)^p}, \quad k, \ell \in \{L, C, R\}$$

where the constant ϵ is used to avoid the denominator vanishing and the constant p weights the smoothness indicator. We use $\epsilon = (\Delta x)^2$ or 10^{-6} and $p = 2$ in the numerical tests. An explicit expression of smoothness indicators is the following:

$$\begin{aligned} \beta_L^i &= (\bar{u}_i - \bar{u}_{i-1})^2, & \beta_R^i &= (\bar{u}_{i+1} - \bar{u}_i)^2, \\ \beta_C^i &= \frac{13}{3}(\bar{u}_{i+1} - 2\bar{u}_i + \bar{u}_{i-1})^2 + \frac{1}{4}(\bar{u}_{i+1} - \bar{u}_{i-1})^2. \end{aligned}$$

We refer to [27] for details on CWENO reconstruction. As a consequence, the reconstruction (2.17) is third order accurate in smooth region and automatically becomes second order accurate in the presence of discontinuity. The final form of the CWENO23 reconstruction $R_i(x)$ is given by

$$(2.19) \quad R_i(x) = R_i^{(0)} + R_i^{(1)}(x - x_i) + \frac{1}{2}R_i^{(2)}(x - x_i)^2,$$

where

$$\begin{aligned} R_i^{(0)} &= \bar{u}_i - \frac{1}{12} \omega_C^i (\bar{u}_{i+1} - 2\bar{u}_i + \bar{u}_{i-1}) \\ R_i^{(1)} &= \omega_L^i \frac{\bar{u}_i - \bar{u}_{i-1}}{\Delta x} + \omega_R^i \frac{\bar{u}_{i+1} - \bar{u}_i}{\Delta x} + \omega_C^i \frac{\bar{u}_{i+1} - \bar{u}_{i-1}}{2\Delta x} \\ R_i^{(2)} &= 2\omega_C^i \frac{\bar{u}_{i+1} - 2\bar{u}_i + \bar{u}_{i-1}}{(\Delta x)^2}. \end{aligned}$$

The CWENO23Z reconstruction also takes the form (2.19), but its non-linear weights are calculated as follows:

$$(2.20) \quad \omega_k^i = \frac{\alpha_k^i}{\sum_\ell \alpha_\ell^i}, \quad \alpha_k^i = C_i \left(1 + \frac{\tau}{\epsilon + \beta_k^i} \right)^p, \quad k, \ell \in \{L, C, R\}$$

where $p \geq 1$ and $\tau = |\beta_R^i - \beta_L^i|$.

Remark 2.4. In D, we prove that the condition (2.12) in Proposition 2.1 is satisfied both for CWENO23 and CWENO23Z if a given u function is smooth enough. This shows that the corresponding reconstruction (2.19) becomes a fourth order accurate reconstruction for smooth solutions.

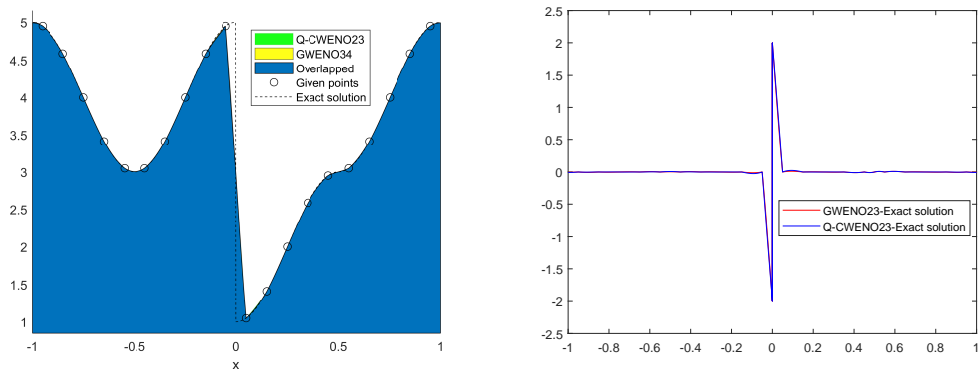
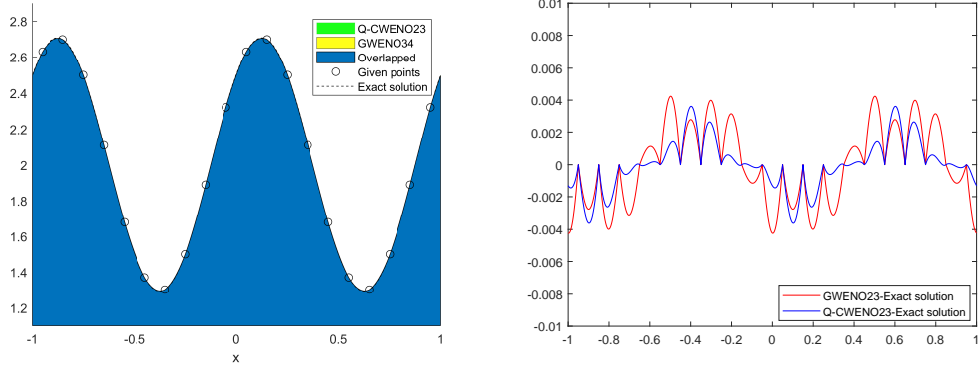


FIGURE 2. Comparison of reconstructions between Q-CWENO23 and GWENO34. In Figs.2a and 2c, dashed lines are exact solutions $\bar{u}_1(x)$, \bar{u}_2x and black circles are given values on grid points of \bar{u}_1x , \bar{u}_2x in (2.21) and (2.22).

Reconstruction	Fig.2a	Fig.2c
Q-CWENO23	6.6613e-16	5.0753e-16
GWENO34	6.6613e-16	9.2766e-04

TABLE 1. Relative conservation errors (2.23) of the reconstruction for \bar{u}_1 (2.21) and \bar{u}_2 (2.22).

In Fig. 2, we compare the proposed conservative reconstruction (2.19) using CWENO23 [29] with a generalized WENO reconstruction originally proposed in [7] in the context of semi-Lagrangian method. We shall denote it by GWENO34 obtained with four points, which achieves fourth order accuracy in the smooth solution. Hereafter we denote by Q-CWENO23 the conservative reconstruction based on CWENO23. To compute solutions with a few points $N = 20$, we set $\epsilon = 1$ for Q-CWENO23. We consider the following sliding average functions on the periodic domain $[-1, 1]$:

$$(2.21) \quad \bar{u}_1(x) = 4 + \sin(2\pi x) + \cos(2\pi x), \quad -1 \leq x < 1,$$

$$(2.22) \quad \bar{u}_2(x) = \begin{cases} 3 + 2 \sin^2(\pi(x - 0.5)), & -1 \leq x < 0 \\ 3 - 2 \sin^2(\pi(x - 0.5)), & 0 \leq x < 0.5 \\ 3 + 2 \sin^2(\pi(x - 0.5)), & 0.5 \leq x < 1. \end{cases}$$

In Fig. 2, one can observe that Q-CWENO23 and GWENO34 show similar results. For a smooth function $\bar{u}_1(x)$ in (2.21), Figs. 2a and 2b implies that errors are relatively small, while for a discontinuous function $\bar{u}_2(x)$ in (2.22), Figs. 2c, 2d show that errors are concentrated near a discontinuity.

In order to clarify the difference between solutions, in Table 1, we report the maximal relative conservation errors between the summation of reconstructed points $Q_{i+\theta}$ and that of given points $\bar{u}_\ell(x_i)$, $\ell = 1, 2$, over $\theta = 0, 0.001, \dots, 0.999$ using the following measure:

$$(2.23) \quad Err_\ell = \frac{\max_\theta |\sum_i Q_{i+\theta} - \sum_i \bar{u}_\ell(x_i)|}{\sum_i \bar{u}_\ell(x_i)}, \quad \ell = 1, 2.$$

From the Table 1, we conclude that Q-CWENO23 recovers the reference summation of $\bar{u}_\ell(x_i)$ for any values of $\theta \in [0, 1]$ even in the presence of a discontinuity. The errors for Q-CWENO23 and GWENO34 are both within machine precision for the smooth function \bar{u}_1 . In this case, the two reconstructions almost coincides the standard Lagrangian interpolation which is conservative. When the function is not smooth as in \bar{u}_2 , Q-CWENO23 is still fully conservative within machine precision, hence it verifies Proposition 2.3. Numerical experiments in which conservation is relevant will be discussed in section 5.

Remark 2.5. As an example for the case $k = 4$, we can use CWENO35 [6] as a basic reconstruction. The explicit form of $R_i^{(ell)}$, $\ell = 0, 1, 2, 3, 4$ is presented in (E).

2.2.2. Positive preserving property. In several circumstances the solution one is looking for is a non negative function. This is the case, for example, of distribution function in kinetic equations. In such cases it may be important to preserve at a discrete level the positivity of the solution. Standard piecewise polynomial reconstructions (linear reconstructions) do not preserve positivity, however several techniques exist in the literature that can be adopted to ensure positivity in the reconstruction ([5, 34]). Here we remark that if the basic reconstruction R is positive preserving, that the sliding average of R will provide a conservative and positivity preserving reconstruction. Given a non-negative basic reconstructions $R_i(x) \geq 0$, obtained from positive cell averages $\bar{u}_i > 0 \forall i$, the positivity of the reconstruction (2.7) directly follows from (2.2). Here we verify this with a numerical example. Let us consider a basic reconstruction R_i , obtained from positive cell averages $\{\bar{u}_i\}$, using the *Positive Flux Conservative* (PFC) technique explained in [18]:

$$(2.24) \quad R_i(x) = R_i^{(0)} + R_i^{(1)}(x - x_i) + \frac{R_i^{(2)}}{2}(x - x_i)^2, \quad x \in [x_{i-1/2}, x_{i+1/2}].$$

Here $R_i^{(0)}$, $R_i^{(1)}$ and $R_i^{(2)}$ are given by

$$\begin{aligned} R_i^{(0)} &= \bar{u}_i - \frac{\varepsilon_i^+(\bar{u}_{i+1} - \bar{u}_i) - \varepsilon_i^-(\bar{u}_i - \bar{u}_{i-1})}{24}, \\ R_i^{(1)} &= \frac{\varepsilon_i^+(\bar{u}_{i+1} - \bar{u}_i) + \varepsilon_i^-(\bar{u}_i - \bar{u}_{i-1})}{2\Delta x}, \\ R_i^{(2)} &= \frac{\varepsilon_i^+(\bar{u}_{i+1} - \bar{u}_i) - \varepsilon_i^-(\bar{u}_i - \bar{u}_{i-1})}{(\Delta x)^2}, \end{aligned}$$

where slope limiters ε_i^+ and ε_i^- are defined by

$$(2.25) \quad \begin{aligned} \varepsilon_i^+ &= \begin{cases} \min(1; 2\bar{u}_i/(\bar{u}_{i+1} - \bar{u}_i)), & \text{if } \bar{u}_{i+1} - \bar{u}_i > 0 \\ \min(1; -2(\bar{u}_\infty - \bar{u}_i)/(\bar{u}_{i+1} - \bar{u}_i)), & \text{if } \bar{u}_{i+1} - \bar{u}_i < 0 \end{cases} \\ \varepsilon_i^- &= \begin{cases} \min(1; 2(\bar{u}_\infty - \bar{u}_i))/(\bar{u}_i - \bar{u}_{i-1})), & \text{if } \bar{u}_i - \bar{u}_{i-1} > 0 \\ \min(1; -2\bar{u}_i/(\bar{u}_i - \bar{u}_{i-1})), & \text{if } \bar{u}_i - \bar{u}_{i-1} < 0 \end{cases}, \end{aligned}$$

with $\bar{u}_\infty := \max_i \bar{u}_i$. This basic reconstruction has been proposed in [18] in order to preserve positivity of the solution and maintain essentially non oscillatory property.

Hereafter we denote by Q-Parabola the reconstruction (2.7) based on (2.24). In Fig. 3, we compare Q-Parabola with Q-CWENO23 reconstructions. For this, we use the following sliding average function on the periodic domain $[-1, 1]$:

$$(2.26) \quad \bar{u}_3(x) = \begin{cases} 10^{-5} + 0.1(1 + \sin(\pi x)), & -0.5 \leq x \leq 0.4 \\ 10^{-5}, & \text{otherwise} \end{cases}.$$

In Fig. 3a and 3b, the difference between two reconstructions appears near $[-0.65, -0.55]$ and $[0.45, 0.55]$. In case of Q-Parabola, the use of positive limiter (2.25) always guarantees the positive reconstructions for any $x \in [-1, 1]$, while very small oscillations appear near discontinuities. On the other hand, although Q-CWENO23 always prevents spurious oscillation, negative solutions may occur depending on the choice of ϵ used for non-linear weights (2.18). In this case, we took $\epsilon = 10^{-6}$, and Eq. (2.18) of CWENO23 returns weights very close to the linear ones on the cell $[-0.6, -0.5]$, which gives negative values on the interval $[-0.65, -0.55]$. We remark that if CWENO23 reconstructions give linear polynomials on two consecutive cells, the corresponding reconstruction (2.7) is to be positive between the two cell centers. Consequently, the suitable choice of ϵ can enable Q-CWENO23 to avoid both negative reconstructions and spurious oscillations. Other possible ways to guarantee the positivity of basic reconstructions are to adopt a linear scaling approach [19, 37, 38] or use positive limiters [14, 17].

Summarizing, our reconstruction works as follows:

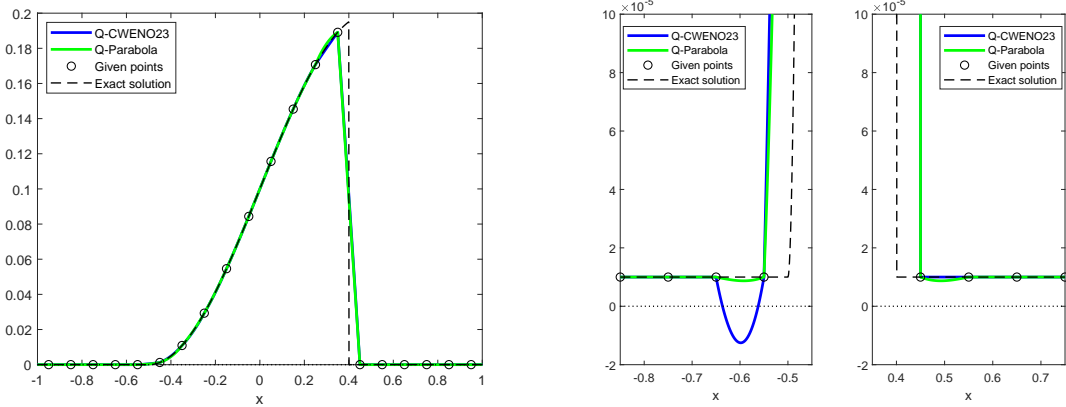
2.2.3. Algorithm for 1D case.

- (1) Given cell average values $\{\bar{u}_i\}_{i \in \mathcal{I}}$ for each $i \in \mathcal{I}$, reconstruct a polynomial of even degree k :

$$R_i(x) = \sum_{\ell=0}^k \frac{R_i^{(\ell)}}{\ell!} (x - x_i)^\ell$$

which is:

- High order accurate in the approximation of smooth $u(x)$:
 - If ℓ is an even integer such that $0 \leq \ell \leq k$: $u_i^{(\ell)} = R_i^{(\ell)} + \mathcal{O}(\Delta x^{k+2-\ell})$.
 - If ℓ is an odd integer such that $0 \leq \ell < k$: $u_i^{(\ell)} - u_{i+1}^{(\ell)} = R_i^{(\ell)} - R_{i+1}^{(\ell)} + \mathcal{O}(\Delta x^{k+2-\ell})$.
- Essentially non-oscillatory.
- Positive preserving.
- Conservative in the sense of cell averages: $\frac{1}{\Delta x} \int_{x_{i-\frac{1}{2}}}^{x_{i+\frac{1}{2}}} R_i(x) dx = \bar{u}_i$.



(A) Comparison of \bar{u}_3 given by (2.26) and its reconstructions.
(B) Comparison of \bar{u}_3 given by (2.26) and its reconstructions on $[-0.85, -0.45]$ and $[0.35, 0.75]$.

FIGURE 3. Comparison of reconstructions between Q-Parabola and Q-CWENO23. Dashed lines are exact solutions $\bar{u}_3(x)$ and black circles are given values on grid points of $\bar{u}_3(x)$ given in (2.26).

(2) Using the obtained values $R_i^{(\ell)}$ for $0 \leq \ell \leq k$, approximate $u(x_{i+\theta})$ with

$$Q_{i+\theta} = \sum_{\ell=0}^k (\Delta x)^\ell \left(\alpha_\ell(\theta) R_i^{(\ell)} + \beta_\ell(\theta) R_{i+1}^{(\ell)} \right),$$

where $\alpha_\ell(\theta)$ and $\beta_\ell(\theta)$ are given in (2.5) and (2.6)

3. CONSERVATIVE RECONSTRUCTION IN 2D

In this section, we introduce the conservative reconstruction technique in two space dimensions, following the one adopted in the previous section. Let $u : \mathbb{R}^2 \rightarrow \mathbb{R}$ be a smooth function and $\bar{u} : \mathbb{R}^2 \rightarrow \mathbb{R}$ be a corresponding sliding average function:

$$\bar{u}(x, y) = \frac{1}{\Delta x \Delta y} \int_{y-\Delta y/2}^{y+\Delta y/2} \int_{x-\Delta x/2}^{x+\Delta x/2} u(x, y) dx dy.$$

Given cell averages on grid points,

$$\frac{1}{\Delta x \Delta y} \int_{I_{i,j}} u(x) dx = \bar{u}_{i,j}, \quad I_{i,j} = [x_{i-\frac{1}{2}}, x_{i+\frac{1}{2}}] \times [y_{j-\frac{1}{2}}, y_{j+\frac{1}{2}}],$$

for each $(i, j) \in \mathcal{I}$, our goal is to approximate the function $\bar{u}(x, y)$. Assume we have a piecewise polynomial reconstruction $R(x, y) = \sum_{i,j} R_{i,j}(x, y) \chi_{i,j}(x, y)$, for $(i, j) \in \mathcal{I}$, where $\chi_{i,j}(x, y)$ is the characteristic function of cell $I_{i,j}$ and each $R_{i,j}(x, y)$ denotes a polynomial of degree k and has the following properties:

(1) It is high order accurate in the approximation of $u(x, y)$:

$$(3.1) \quad u(x, y) = R_{i,j}(x, y) + \mathcal{O}(h^{k+1}), \quad (x, y) \in I_{i,j},$$

where $\Delta x, \Delta y = \mathcal{O}(h)$.

(2) It is conservative in the sense of cell averages:

$$\frac{1}{\Delta x \Delta y} \int_{y_{j-\frac{1}{2}}}^{y_{j+\frac{1}{2}}} \int_{x_{i-\frac{1}{2}}}^{x_{i+\frac{1}{2}}} R_{i,j}(x, y) dx dy = \bar{u}_{i,j}.$$

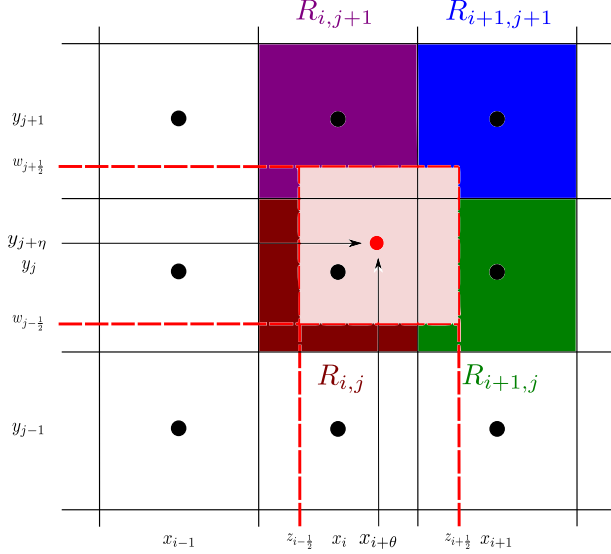


FIGURE 4. Description of two-dimensional conservative reconstruction

We start from a polynomial of degree k , $R_{i,j}(x, y)$:

$$(3.2) \quad R_{i,j}(x, y) = \sum_{|\ell|=0}^k \frac{R_{i,j}^{(\ell)}}{\ell_1! \ell_2!} (x - x_i)^{\ell_1} (y - y_j)^{\ell_2},$$

where we use a multi index $\ell = (\ell_1, \ell_2)$. Consider a cell $I_{i,j}^{\theta,\eta}$ whose center is $(x_{i+\theta}, y_{j+\eta})$ for some $\theta, \eta \in [0, 1]$. In Fig. 4, we note that $(x_{i+\theta}, y_{j+\eta})$ lies inside one of $I_{i,j}, I_{i+1,j}, I_{i,j+1}, I_{i+1,j+1}$. Let us denote a cell $I_{i+\theta,j+\eta} := [z_{i-\frac{1}{2}}, z_{i+\frac{1}{2}}] \times [w_{j-\frac{1}{2}}, w_{j+\frac{1}{2}}]$ and a point $(x_{i+\theta}, y_{j+\eta}) := (x_i + \theta \Delta x, y_j + \eta \Delta y)$. Now, we approximate $\bar{u}(x_{i+\theta}, y_{j+\eta})$ by

$$\begin{aligned} \bar{u}(x_{i+\theta}, y_{j+\eta}) &\approx \frac{1}{\Delta x \Delta y} \int_{w_{j-\frac{1}{2}}}^{w_{j+\frac{1}{2}}} \int_{z_{i-\frac{1}{2}}}^{z_{i+\frac{1}{2}}} R(x, y) dx dy \\ &= \frac{1}{\Delta x \Delta y} \int_{w_{j-\frac{1}{2}}}^{y_{j+\frac{1}{2}}} \int_{z_{i-\frac{1}{2}}}^{x_{i+\frac{1}{2}}} R_{i,j}(x, y) dx dy + \frac{1}{\Delta x \Delta y} \int_{w_{j-\frac{1}{2}}}^{y_{j+\frac{1}{2}}} \int_{x_{i+\frac{1}{2}}}^{z_{i+\frac{1}{2}}} R_{i+1,j}(x, y) dx dy \\ &\quad + \frac{1}{\Delta x \Delta y} \int_{y_{j+\frac{1}{2}}}^{w_{j+\frac{1}{2}}} \int_{z_{i-\frac{1}{2}}}^{x_{i+\frac{1}{2}}} R_{i,j+1}(x, y) dx dy + \frac{1}{\Delta x \Delta y} \int_{y_{j+\frac{1}{2}}}^{w_{j+\frac{1}{2}}} \int_{x_{i+\frac{1}{2}}}^{z_{i+\frac{1}{2}}} R_{i+1,j+1}(x, y) dx dy. \end{aligned}$$

The first integral becomes

$$\begin{aligned} \frac{1}{\Delta x \Delta y} \int_{w_{j-\frac{1}{2}}}^{y_{j+\frac{1}{2}}} \int_{z_{i-\frac{1}{2}}}^{x_{i+\frac{1}{2}}} R_{i,j}(x, y) dx dy &= \frac{1}{\Delta x \Delta y} \sum_{|\ell|=0}^k R_{i,j}^{(\ell)} \int_{y_{j-\frac{1}{2}}+\eta}^{y_{j+\frac{1}{2}}} \int_{x_{i-\frac{1}{2}}+\theta}^{x_{i+\frac{1}{2}}} \frac{1}{\ell_1! \ell_2!} (x - x_i)^{\ell_1} (y - y_j)^{\ell_2} dx dy \\ &= \sum_{|\ell|=0}^k R_{i,j}^{(\ell)} \left(\frac{1}{\Delta x} \int_{x_{i-\frac{1}{2}}+\theta}^{x_{i+\frac{1}{2}}} \frac{(x - x_i)^{\ell_1}}{\ell_1!} dx \right) \left(\frac{1}{\Delta y} \int_{y_{j-\frac{1}{2}}+\eta}^{y_{j+\frac{1}{2}}} \frac{(y - y_j)^{\ell_2}}{\ell_2!} dy \right) \\ &= \sum_{|\ell|=0}^k (\Delta)^{\ell} \alpha_{\ell_1}(\theta) \alpha_{\ell_2}(\eta) R_{i,j}^{(\ell)} \end{aligned}$$

where $(\Delta)^\ell = (\Delta x)^{\ell_1}(\Delta y)^{\ell_2}$. Similarly, we obtain

$$\begin{aligned} \frac{1}{\Delta x \Delta y} \int_{w_{j-\frac{1}{2}}}^{y_{j+\frac{1}{2}}} \int_{x_{i+\frac{1}{2}}}^{z_{i+\frac{1}{2}}} R_{i+1,j}(x, y) dx dy &= \sum_{|\ell|=0}^k (\Delta)^\ell \beta_{\ell_1}(\theta) \alpha_{\ell_2}(\eta) R_{i+1,j}^{(\ell)}, \\ \frac{1}{\Delta x \Delta y} \int_{y_{j+\frac{1}{2}}}^{w_{j+\frac{1}{2}}} \int_{z_{i-\frac{1}{2}}}^{x_{i+\frac{1}{2}}} R_{i,j+1}(x, y) dx dy &= \sum_{|\ell|=0}^k (\Delta)^\ell \alpha_{\ell_1}(\theta) \beta_{\ell_2}(\eta) R_{i,j+1}^{(\ell)}, \\ \frac{1}{\Delta x \Delta y} \int_{y_{j+\frac{1}{2}}}^{w_{j+\frac{1}{2}}} \int_{x_{i+\frac{1}{2}}}^{z_{i+\frac{1}{2}}} R_{i+1,j+1}(x, y) dx dy &= \sum_{|\ell|=0}^k (\Delta)^\ell \beta_{\ell_1}(\theta) \beta_{\ell_2}(\eta) R_{i+1,j+1}^{(\ell)}. \end{aligned}$$

Denoting the approximation of $\bar{u}(x_{i+\theta}, y_{j+\theta})$ by $Q_{i+\theta, j+\theta}$, we write it as

$$\begin{aligned} (3.3) \quad Q_{i+\theta, j+\theta} &= \sum_{|\ell|=0}^k (\Delta)^\ell \left(\alpha_{\ell_1}(\theta) \alpha_{\ell_2}(\eta) R_{i,j}^{(\ell)} + \beta_{\ell_1}(\theta) \alpha_{\ell_2}(\eta) R_{i+1,j}^{(\ell)} \right. \\ &\quad \left. + \alpha_{\ell_1}(\theta) \beta_{\ell_2}(\eta) R_{i,j+1}^{(\ell)} + \beta_{\ell_1}(\theta) \beta_{\ell_2}(\eta) R_{i+1,j+1}^{(\ell)} \right), \end{aligned}$$

where the explicit forms of $\alpha_{\ell_1}(\theta)$, $\alpha_{\ell_2}(\eta)$, $\beta_{\ell_1}(\theta)$, $\beta_{\ell_2}(\eta)$ are given in (2.5) and (2.6).

3.1. General Properties. In the following proposition, as in Proposition 2.3, we show that the approximation $Q_{i+\theta, j+\theta}$ is of order $(k+2)$ of accuracy for an even integer $k \geq 0$. For simplicity, we assume $\Delta x, \Delta y = h > 0$.

Proposition 3.1. *Let $k \geq 0$ be an even integer and u be smooth enough so that a piecewise polynomial $R(x, y) = \sum_{i,j} R_{i,j}(x, y) \chi_{i,j}$ satisfies*

$$\begin{aligned} (3.4) \quad u_{i,j}^{(\ell)} &= R_{i,j}^{(\ell)} + \mathcal{O}(h^{k+2-|\ell|}), \quad \ell \in A \\ u_{i,j}^{(\ell)} - u_{i+1,j}^{(\ell)} &= R_{i,j}^{(\ell)} - R_{i+1,j}^{(\ell)} + \mathcal{O}(h^{k+2-|\ell|}), \quad \ell \in B \\ u_{i,j}^{(\ell)} - u_{i,j+1}^{(\ell)} &= R_{i,j}^{(\ell)} - R_{i,j+1}^{(\ell)} + \mathcal{O}(h^{k+2-|\ell|}), \quad \ell \in C \end{aligned}$$

where the set A, B and C are defined

$$\begin{aligned} (3.5) \quad A &= \{\ell : |\ell| = \text{even}, \quad 0 \leq |\ell| \leq k\}, \\ B &= \{\ell : \ell_1 = \text{odd}, \quad \ell_2 = \text{even}, \quad 0 \leq |\ell| \leq k\}, \\ C &= \{\ell : \ell_1 = \text{even}, \quad \ell_2 = \text{odd}, \quad 0 \leq |\ell| \leq k\}. \end{aligned}$$

Then the reconstruction $Q_{i+\theta, j+\theta}$ gives a $(k+2)$ -th-order approximation of sliding averages $\bar{u}_{i+\theta, j+\theta}$ for any $\theta, \eta \in [0, 1]$.

Proof. For detailed proof, see F. □

The conservation property also holds in the 2D reconstruction (3.3):

Proposition 3.2. *Assume that $R_{i,j}(x, y)$ satisfies*

$$\frac{1}{\Delta x \Delta y} \int_{y_{j-\frac{1}{2}}}^{y_{j+\frac{1}{2}}} \int_{x_{i-\frac{1}{2}}}^{x_{i+\frac{1}{2}}} R_{i,j}(x, y) dx dy = \bar{u}_{i,j}, \quad (i, j) \in \mathcal{I}.$$

Then, for periodic functions $\bar{u}(x, y)$ with period $(L, L) = (Nh, Nh)$, $N \in \mathbb{N}$

$$\sum_{1 \leq i, j \leq N} Q_{i+\theta, j+\theta} = \sum_{1 \leq i, j \leq N} \bar{u}_{i,j},$$

for any $\theta, \eta \in [0, 1]$.

Proof. The proof is similar to the one dimensional case. □

3.1.1. Algorithm for 2D case.

- (1) Given cell average values $\{\bar{u}_{i,j}\}_{(i,j) \in \mathcal{I}}$ for each $(i,j) \in \mathcal{I}$, reconstruct a polynomial of degree k :

$$R_{i,j}(x,y) = \sum_{|\ell|=0}^k \frac{R_{i,j}^{(\ell)}}{\ell_1! \ell_2!} (x-x_i)^{\ell_1} (y-y_j)^{\ell_2}$$

which is:

- High order accurate in the approximation of $u(x)$:

$$\begin{aligned} u_{i,j}^{(\ell)} &= R_{i,j}^{(\ell)} + \mathcal{O}(h^{k+2-|\ell|}), \quad \ell \in A \\ u_{i,j}^{(\ell)} - u_{i+1,j}^{(\ell)} &= R_{i,j}^{(\ell)} - R_{i+1,j}^{(\ell)} + \mathcal{O}(h^{k+2-|\ell|}), \quad \ell \in B \\ u_{i,j}^{(\ell)} - u_{i,j+1}^{(\ell)} &= R_{i,j}^{(\ell)} - R_{i,j+1}^{(\ell)} + \mathcal{O}(h^{k+2-|\ell|}), \quad \ell \in C \end{aligned}$$

where sets A, B, C are defined in (3.5).

- Essentially non-oscillatory.
- Positive preserving.
- Conservative in the sense of cell averages: $\frac{1}{\Delta x \Delta y} \int_{y_{j-\frac{1}{2}}}^{y_{j+\frac{1}{2}}} \int_{x_{i-\frac{1}{2}}}^{x_{i+\frac{1}{2}}} R_{i,j}(x,y) dx dy = \bar{u}_{i,j}$.

- (2) Using the obtained values $R_{i,j}^{(\ell)}$ for $0 \leq |\ell| \leq k$, approximate $\bar{u}(x_{i+\theta}, y_{j+\eta})$ with

$$\begin{aligned} Q_{i+\theta,j+\eta} = \sum_{|\ell|=0}^k (\Delta)^{\ell} \left(\alpha_{\ell_1}(\theta) \alpha_{\ell_2}(\eta) R_{i,j}^{(\ell)} + \beta_{\ell_1}(\theta) \alpha_{\ell_2}(\eta) R_{i+1,j}^{(\ell)} \right. \\ \left. + \alpha_{\ell_1}(\theta) \beta_{\ell_2}(\eta) R_{i,j+1}^{(\ell)} + \beta_{\ell_1}(\theta) \beta_{\ell_2}(\eta) R_{i+1,j+1}^{(\ell)} \right), \end{aligned}$$

where $\alpha_{\ell_1}(\theta)$, $\alpha_{\ell_2}(\eta)$, $\beta_{\ell_1}(\theta)$, $\beta_{\ell_2}(\eta)$ are computable using (2.5) and (2.6).

4. SEMI-LAGRANGIAN SCHEMES FOR HYPERBOLIC SYSTEMS WITH RELAXATION

In this section, as an application of the conservative reconstruction (2.7) and (3.3), we consider semi-Lagrangian methods to semi-linear hyperbolic relaxation systems. Two semi-linear hyperbolic relaxation system, namely, Xin-Jin system [23] and Broadwell model [3], where a relaxation parameter κ makes each system stiff as $\kappa \rightarrow 0$.

In order to treat the stiffness, we shall use L-stable s -stage DIRK methods or L-stable linear multi-step methods (in particular BDF methods) [20]. These methods provide a balanced performance between stability and efficiency.

From now on, we focus on L-stable s -stage DIRK methods represented by Butcher's tables:

$$\begin{array}{c|c} c & A \\ \hline & b^T \end{array}$$

where $A = [a_{k\ell}]$ is a $s \times s$ lower triangle matrix such that $a_{k\ell} = 0$ for $\ell > k$, $c = (c_1, \dots, c_s)^T$ and $b = (b_1, \dots, b_s)^T$ are coefficient vectors. (For BDF based methods, we refer to G.1.)

In order to guarantee L-stability, here we make use of *stiffly accurate* schemes (SA), i.e. schemes for which the last row of matrix A is equal to the vector of weights $a_{sj} = b_j$, $j = 1, \dots, s$. This will ensure that the absolute stability function vanishes at infinity. As a consequence, an A-stable scheme which is SA is also L-stable, [20].

In the numerical tests for each order of accuracy, we will use the following high-order L-stable DIRK methods:

- second-order DIRK method (DIRK2) [21],

$$(4.1) \quad \begin{array}{c|ccc} \alpha & \alpha & 0 \\ \hline 1 & 1-\alpha & \alpha \\ & 1-\alpha & \alpha \end{array}, \quad \alpha = 1 - \frac{\sqrt{2}}{2}.$$

- third-order DIRK method (DIRK43) [25],

$$(4.2) \quad \begin{array}{c|ccccc} 0 & 0 & 0 & 0 & 0 \\ \hline 2\gamma & \gamma & \gamma & 0 & 0 \\ c & c-\delta-\gamma & \delta & \gamma & 0 \\ \hline 1 & 1-b_2-b_3-\gamma & b_2 & b_3 & \gamma \\ \hline & 1-b_2-b_3-\gamma & b_2 & b_3 & \gamma \end{array}$$

with $\gamma = \frac{1767732205903}{4055673282236}$, $c = \frac{3}{5}$, $b_2 = -\frac{4482444167858}{7529755066697}$, $b_3 = \frac{11266239266428}{11593286722821}$, $\delta = -\frac{640167445237}{6845629431997}$.

4.1. Xin-Jin relaxation system. Consider a simplified Xin-Jin relaxation system [23]:

$$(4.3) \quad \begin{aligned} \frac{\partial u}{\partial t} + \sum_{i=1}^d \frac{\partial v}{\partial x_i} &= 0, \\ \frac{\partial v}{\partial t} + a^2 \sum_{i=1}^d \frac{\partial u}{\partial x_i} &= \frac{1}{\kappa} (F(u) - v), \end{aligned}$$

where d denotes the dimension of space variable. When κ goes to zero, the solution in (4.3) converges to

$$(4.4) \quad \frac{\partial u}{\partial t} + \sum_{i=1}^d \frac{\partial F(u)}{\partial x_i} = 0, \quad v = F(u).$$

provided that the subcharacteristic condition is satisfied, i.e., $\max_u |F'(u)| \leq |a|$ (see [11]). For example, taking $F(u) = u^2/2$, the system (4.4) formally becomes the Burgers equation:

$$(4.5) \quad \frac{\partial u}{\partial t} + \sum_{i=1}^d u \frac{\partial u}{\partial x_i} = 0, \quad v = \frac{u^2}{2}.$$

In this equation, shocks may appear in a finite time and we need to impose our scheme to be conservative to capture the positions of such shocks correctly. We treat this shock problem in section 5.

4.1.1. Semi-Lagrangian scheme for Xin-Jin relaxation system. Using $u - v = f$ and $u + v = g$, we rewrite (4.3) as

$$(4.6) \quad \begin{aligned} \frac{\partial f}{\partial t} - \sum_{i=1}^d \frac{\partial f}{\partial x_i} &= -\frac{1}{\kappa} \left[F\left(\frac{g+f}{2}\right) - \frac{g-f}{2} \right] \\ \frac{\partial g}{\partial t} + \sum_{i=1}^d \frac{\partial g}{\partial x_i} &= -\frac{1}{\kappa} \left[\frac{g-f}{2} - F\left(\frac{g+f}{2}\right) \right]. \end{aligned}$$

Based on this, we consider its Lagrangian formulation:

$$(4.7) \quad \begin{aligned} \frac{df}{dt}(X_1(t), t) &= -\frac{1}{\kappa} \left[F\left(\frac{g+f}{2}\right) - \frac{g-f}{2} \right](X_1(t), t), \quad \frac{dX_1}{dt} = -\mathbb{1} \\ \frac{dg}{dt}(X_2(t), t) &= -\frac{1}{\kappa} \left[\frac{g-f}{2} - F\left(\frac{g+f}{2}\right) \right](X_2(t), t), \quad \frac{dX_2}{dt} = \mathbb{1}, \end{aligned}$$

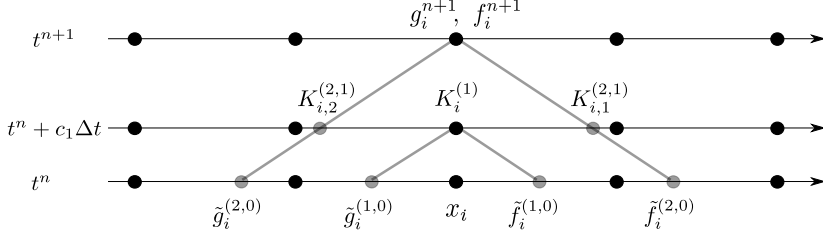


FIGURE 5. Schematic of DIRK2 based SL method for Xin-Jin model. Gray circles are points where reconstruction is required.

where $\mathbb{1} = (1, \dots, 1) \in \mathbb{N}^d$ and $X_1(t^{n+1}) = X_2(t^{n+1}) = x_i \in \mathbb{R}^d$.

To clarify high order methods for (4.7), we introduce the following notation:

- The ℓ -th stage values of f, g along the backward-characteristics which come from x_i with characteristic speed $-1, 1$ at time $t^n + c_k \Delta t$:

$$\tilde{f}_i^{(k,\ell)} \approx f(x_i + (c_k - c_\ell)\Delta t, t^n + c_\ell \Delta t), \quad \tilde{g}_i^{(k,\ell)} \approx g(x_i - (c_k - c_\ell)\Delta t, t^n + c_\ell \Delta t)$$

where " \approx " implies the necessity of suitable reconstructions. We also denote k -th stage value of f, g on x_i by

$$f_i^{(k)} = f(x_i, t^n + c_k \Delta t), \quad g_i^{(k)} = g(x_i, t^n + c_k \Delta t)$$

for $1 \leq k \leq s$ where $f_i^{(k)} = u_i^{(k)} - v_i^{(k)}$ and $g_i^{(k)} = u_i^{(k)} + v_i^{(k)}$.

- For $\ell = 0$, we set $c_\ell = 0$ hence

$$(4.8) \quad \tilde{f}_i^{(k,0)} \approx f(x_i + c_k \Delta t, t^n), \quad \tilde{g}_i^{(k,0)} \approx g(x_i - c_k \Delta t, t^n).$$

- Define a RK flux function by $K_1 := F(u) - v$, $K_2 := -K_1$, then

$$K_{i,j}^{(k,\ell)} \approx K_j(x_i - \lambda_j(c_k - c_\ell)\Delta t, t^n + c_\ell \Delta t), \quad j = 1, 2$$

where $\lambda_1 = -1, \lambda_2 = 1$ and $K_{i,j}^{(k)} = K_j(x_i, t^n + c_k \Delta t)$.

With these, we can represent a high order method compactly. Applying a L-stable s -stage DIRK method to system (4.7), we have k -stage values

$$(4.9) \quad \begin{aligned} f_i^{(k)} &= \tilde{f}_i^{(k,0)} - \frac{\Delta t}{\kappa} \sum_{\ell=1}^s a_{k\ell} K_{i,1}^{(k,\ell)}, \\ g_i^{(k)} &= \tilde{g}_i^{(k,0)} - \frac{\Delta t}{\kappa} \sum_{\ell=1}^s a_{k\ell} K_{i,2}^{(k,\ell)}, \end{aligned}$$

for $k = 1, \dots, s$. Since we only consider SA DIRK schemes, the s -stage values become the numerical solutions: $f_i^{n+1} = f_i^{(s)}$ and $g_i^{n+1} = g_i^{(s)}$. It is worth mentioning that each k -stage value can be computed in an explicit way. After summing and subtracting two equations in (4.9), we obtain

$$(4.10) \quad \begin{aligned} u_i^{(k)} &= \frac{\tilde{g}_i^{(k,0)} + \tilde{f}_i^{(k,0)}}{2} - \frac{\Delta t}{2\kappa} \sum_{\ell=1}^{k-1} a_{k\ell} \left(K_{i,1}^{(k,\ell)} + K_{i,2}^{(k,\ell)} \right), \\ v_i^{(k)} &= \frac{\tilde{g}_i^{(k,0)} - \tilde{f}_i^{(k,0)}}{2} - \frac{\Delta t}{2\kappa} \left(\sum_{\ell=1}^{k-1} a_{k\ell} \left(K_{i,2}^{(k,\ell)} - K_{i,1}^{(k,\ell)} \right) \right) + \frac{a_{kk}\Delta t}{\kappa} \left(F(u_i^{(k)}) - v_i^{(k)} \right). \end{aligned}$$

Here we first compute $u_i^{(k)}$, and use it obtain $v_i^{(k)}$. Now we illustrate our L-stable DIRK schemes as follows: (A schematic for DIRK2 based scheme is given in Fig 5.)

4.1.2. *Algorithm of s-stage L-stable DIRK method.* For $k = 1, \dots, s$.

- (1) Interpolate $\tilde{f}_i^{(k,0)}$ and $\tilde{g}_i^{(k,0)}$ on $x_i + c_k \Delta t$ and $x_i - c_k \Delta t$ from $\{f_i^n\}$ and $\{g_i^n\}$, respectively.
- (2) Compute $u_i^{(k)}$ and $v_i^{(k)}$ from (4.10).
- (3) Compute:

$$(4.11) \quad f_i^{(k)} = u_i^{(k)} - v_i^{(k)}, \quad g_i^{(k)} = u_i^{(k)} + v_i^{(k)}$$

- (4) If $k < s$, compute

$$K_{i,1}^{(k)} = F(u_i^{(k)}) - v_i^{(k)}, \quad K_{i,2}^{(k)} = -K_{i,1}^{(k)}$$

and, for $\ell = k + 1, \dots, s$, interpolate

$$\begin{aligned} K_{i,1}^{(\ell,k)} &\text{ on } x_i + (c_\ell - c_k) \Delta t \text{ from } \{K_{i,1}^{(k)}\}, \\ K_{i,2}^{(\ell,k)} &\text{ on } x_i - (c_\ell - c_k) \Delta t \text{ from } \{K_{i,2}^{(k)}\}. \end{aligned}$$

- (5) Compute numerical solution: $f_i^{n+1} = f_i^{(s)}$ and $g_i^{n+1} = g_i^{(s)}$.

For any term where reconstruction is required, we use the formula (2.7) based on the CWENO reconstructions.

Remark 4.1. In the Algorithm 4.1.2, using the implicit Euler method for $s = 1$ and taking a limit $\kappa \rightarrow 0$ in (4.10), we obtain

$$(4.12) \quad u_i^{n+1} = \frac{\tilde{g}_i^{(1,0)} + \tilde{f}_i^{(1,0)}}{2}, \quad v_i^{n+1} = F(u_i^{n+1}),$$

for all $n \geq 0$ regardless of initial data. Now assume that $\Delta t = \Delta x$, and we combine (4.12) with (4.8), and (4.11) for $k = 1$ obtaining

$$u_i^{n+1} = \frac{1}{2} (u_{i+1}^n + u_{i-1}^n) - \frac{1}{2} (F(u_{i+1}^n) - F(u_{i-1}^n)).$$

This is the LaxFriedrichs method of the conservation law in (4.4) with $\Delta t = \Delta x$.

4.2. **Broadwell model.** Next example is the Broadwell model of kinetic theory [3]:

$$(4.13) \quad \begin{aligned} \partial_t f + \partial_x f &= \frac{1}{\kappa} Q \\ \partial_t g - \partial_x g &= \frac{1}{\kappa} Q \\ \partial_t h &= -\frac{1}{\kappa} Q. \end{aligned}$$

where $Q = h^2 - fg$. Introducing the fluid dynamic moment variables dentity ρ , momentum m , and velocity u and an additional variable z as follows:

$$(4.14) \quad \rho = f + 2h + g, \quad m = f - g, \quad z = f + g,$$

the system (4.13) can be rewritten as

$$(4.15) \quad \begin{aligned} \partial_t \rho + \partial_x m &= 0 \\ \partial_t m + \partial_x z &= 0 \\ \partial_t z + \partial_x m &= \frac{1}{2\kappa} (\rho^2 - 2\rho z + m^2). \end{aligned}$$

Note that the original variables can be recovered by

$$f = \frac{z + m}{2}, \quad g = \frac{z - m}{2}, \quad h = \frac{\rho - z}{2}.$$

As $\kappa \rightarrow 0$, one can see that z goes to a local equilibrium

$$z \rightarrow z_E(\rho, m) := \frac{1}{2\rho} (\rho^2 + m^2) = \frac{1}{2} (\rho + \rho u^2)$$

and the system (4.15) becomes the Euler equations:

$$(4.16) \quad \begin{aligned} \partial_t \rho + \partial_x m &= 0 \\ \partial_t m + \partial_x \left(\frac{1}{2} (\rho + \rho u^2) \right) &= 0. \end{aligned}$$

4.2.1. Semi-Lagrangian scheme for the Broadwell model. Here, we consider again DIRK methods based on Tables (4.1)-(4.2). The schemes are also explicitly solvable with algebraic computations. (For BDF methods, we refer to (G.2).)

Let us denote k -th stage values by $f_i^{(k)}, g_i^{(k)}, h_i^{(k)}$, $1 \leq k \leq s$, and introduce the following notation:

$$\begin{aligned} Q_i^{(k)} &= (h_i^{(k)})^2 - f_i^{(k)} g_i^{(k)}, \\ Q_{i,1}^{(k,\ell)} &\approx Q(x_i - (c_k - c_\ell)\Delta t, t^n + c_\ell\Delta t), \quad Q_{i,2}^{(k,\ell)} \approx Q(x_i + (c_k - c_\ell)\Delta t, t^n + c_\ell\Delta t), \\ f_i^{(k,\ell)} &\approx f(x_i - (c_k - c_\ell)\Delta t, t^n + c_\ell\Delta t), \quad g_i^{(k,\ell)} \approx g(x_i - (c_k - c_\ell)\Delta t, t^n + c_\ell\Delta t). \end{aligned}$$

Applying a s -stage DIRK method to (4.13), we can write k -th stage values in a compact form:

$$(4.17) \quad \begin{aligned} f_i^{(k)} &= F_i^{(k)} + \frac{a_{kk}\Delta t}{\kappa} Q_i^{(k)}, \quad F_i^{(k)} := f_i^{(k,0)} + \frac{\Delta t}{\kappa} \sum_{\ell=1}^{k-1} a_{k\ell} Q_{i,1}^{(k,\ell)} \\ g_i^{(k)} &= G_i^{(k)} + \frac{a_{kk}\Delta t}{\kappa} Q_i^{(k)}, \quad G_i^{(k)} := g_i^{(k,0)} + \frac{\Delta t}{\kappa} \sum_{\ell=1}^{k-1} a_{k\ell} Q_{i,2}^{(k,\ell)} \\ h_i^{(k)} &= H_i^{(k)} - \frac{a_{kk}\Delta t}{\kappa} Q_i^{(k)}, \quad H_i^{(k)} := h_i^n - \frac{\Delta t}{\kappa} \sum_{\ell=1}^{k-1} a_{k\ell} Q_i^{(\ell)}, \end{aligned}$$

for $k = 1, 2, \dots, s$. Here the SA property also implies $f_i^{n+1} = f_i^{(s)}$, $g_i^{n+1} = g_i^{(s)}$ and $h_i^{n+1} = h_i^{(s)}$.

Now, we describe the algorithm:

4.2.2. Algorithm of s -stage L-stable DIRK method. For $k = 1, \dots, s$, iterate the following procedures:

- (1) Reconstruct $f_i^{(k,0)}$ and $g_i^{(k,0)}$ on $x_i - c_k \Delta t$ and $x_i + c_k \Delta t$ from $\{f_i^n\}$ and $\{g_i^n\}$, respectively.
- (2) Reconstruct $Q_{i,1}^{(k,\ell)}$ and $Q_{i,2}^{(k,\ell)}$ for $\ell = 1, \dots, k-1$ from $\{Q_i^{(\ell)}\}$ (skip this if $k=1$).
- (3) Compute $F_i^{(k)}$, $G_i^{(k)}$ and $H_i^{(k)}$ using (4.17).
- (4) Solve

$$(4.18) \quad f_i^{(k)} = F_i^{(k)} + \frac{a_{kk}\Delta t}{\kappa} Q_i^{(k)}, \quad g_i^{(k)} = G_i^{(k)} + \frac{a_{kk}\Delta t}{\kappa} Q_i^{(k)}, \quad h_i^{(k)} = H_i^{(k)} - \frac{a_{kk}\Delta t}{\kappa} Q_i^{(k)}$$

for

$$(4.19) \quad \begin{aligned} h_i^{(k)} &= \frac{a_{kk}\Delta t(H_i^{(k)} + F_i^{(k)})(H_i^{(k)} + G_i^{(k)}) + \kappa H_i^{(k)}}{a_{kk}\Delta t(G_i^{(k)} + 2H_i^{(k)} + F_i^{(k)}) + \kappa}, \\ f_i^{(k)} &= H_i^{(k)} + F_i^{(k)} - h_i^{(k)}, \quad g_i^{(k)} = H_i^{(k)} + G_i^{(k)} - h_i^{(k)}. \end{aligned}$$

Remark 4.2. In Algorithm 4.2.2, consider the case $s = 1$ for implicit Euler method. Under the assumption $\Delta t = \Delta x$, the relaxation limit $\kappa \rightarrow 0$ in (4.19) gives

$$(4.20) \quad \begin{aligned} h_i^{n+1} &= \frac{(h_i^n + f_{i-1}^n)(h_i^n + g_{i+1}^n)}{g_{i+1}^n + 2h_i^n + f_{i-1}^n}, \\ f_i^{n+1} &= h_i^n + f_i^{(1,0)} - h_i^{n+1}, \quad g_i^{n+1} = h_i^n + g_i^{(1,0)} - h_i^{n+1}. \end{aligned}$$

This limiting scheme coincides with the relaxation scheme in [24] applied to the Broadwell model. Also, using the relation (4.14), we can rewrite it as follows:

$$\begin{aligned}\rho_i^{n+1} &= \rho_i^n - \frac{1}{2} (m_{i+1}^n - m_{i-1}^n) + \frac{1}{2} (z_{i-1}^n - 2z_i^n + z_{i+1}^n), \\ m_i^{n+1} &= \frac{1}{2} (m_{i+1}^n + m_{i-1}^n) - \frac{1}{2} (z_{i+1}^n - z_{i-1}^n), \\ z_i^{n+1} &= \frac{(\rho_i^{n+1})^2 + (m_i^{n+1})^2}{2\rho_i^{n+1}}.\end{aligned}$$

We note that the scheme projects numerical solutions to equilibrium after one time step.

5. NUMERICAL TESTS

Our main interest is to confirm the performance of the proposed reconstruction in one and two dimensions. For numerical experiments, we consider the reconstruction (2.7) and (3.3) based on CWENO reconstructions. This section is divided into three parts: 1D Xin-Jin model (4.3), 1D Broadwell model (4.13) and 2D Xin-Jin model (4.3). For each system, we check the accuracy of the corresponding semi-Lagrangian schemes and consider the related shock problems which arise in the relaxation limit $\kappa \rightarrow 0$. For numerical tests, we use the CFL number defined by $\text{CFL} = \frac{\Delta t}{\Delta x}$ using uniform grid points based on Δx and Δt . For 2D, we use $\text{CFL} = \frac{\Delta t}{\Delta x} = \frac{\Delta t}{\Delta y}$.

5.1. 1D case for Xin-Jin model. Here tests are based on the numerical method in Algorithm 4.1.2. Note that we adopt $F(u) = u^2/2$.

5.1.1. Accuracy test. We take well-prepared initial data up to first order in κ [2]:

$$(5.1) \quad u_0(x) = 0.7 + 0.2 \sin(\pi x), \quad v_0(x) = \frac{u_0^2(x)}{2} + \kappa (u_0^2(x) - 1) \partial_x u_0(x),$$

where periodic boundary conditions are imposed on $x \in [-1, 1]$. In the limit $\kappa \rightarrow 0$ with $F(u) = u^2/2$, system (4.3) becomes the Burgers equation where shock appears after the positive minimum time: $T_b := \inf_{u'_0 < 0} \left\{ -\frac{1}{u'_0(x)} \right\}$. In view of this, we take a final time as $T^f = 1$ which is less than the breaking time $T_b = 5/\pi \approx 1.5915$. In this test, we use several values of $\text{CFL} = \Delta t / \Delta x < 1$. We remark that the subcharacteristic condition $\max_u |F'(u)| < 1$ is always satisfied. In Fig. 6, a DIRK2 based method attains its desired accuracy between 2 and 3. In the case of DIRK43 method, it attains its desired accuracy between 3 and 5 except for some order reductions which appear in the intermediate regimes. We remark that the spatial errors are dominant for small CFL numbers, which make it easy to observe the order of spatial reconstructions.

5.1.2. Shock tests. To confirm the conservation property of the proposed reconstruction in shock problems, we here compare numerical solutions obtained by conservative semi-Lagrangian schemes with non-conservative ones.

- **Smooth initial data.** We first take the an smooth initial data

$$(5.2) \quad u_0(x) = 0.7 + 0.2 \sin(\pi x), \quad v_0(x) = \frac{u_0^2(x)}{2},$$

where periodic boundary condition is imposed on $x \in [-1, 1]$. We use grid points of $N_x = 160$ up to final time $T^f = 4$. Each time step is taken by $\Delta t = \text{CFL} \Delta x$. For each time $t = t^n$, we compute the conservation error using

$$E_{con}^n := \frac{|\sum_i u_i^n \Delta x - \sum_i u_i^0 \Delta x|}{\sum_i u_i^0 \Delta x}.$$

In Fig. 7, we compare the numerical solutions obtained from our reconstruction, linear interpolation (first order scheme), GWENO34 and GWENO46 [7] with the reference solution in [36]. We observe that the use of our reconstruction and linear interpolation leads to correct shock position. Also, the corresponding conservative errors show very small change as time flows. In contrast, conservation

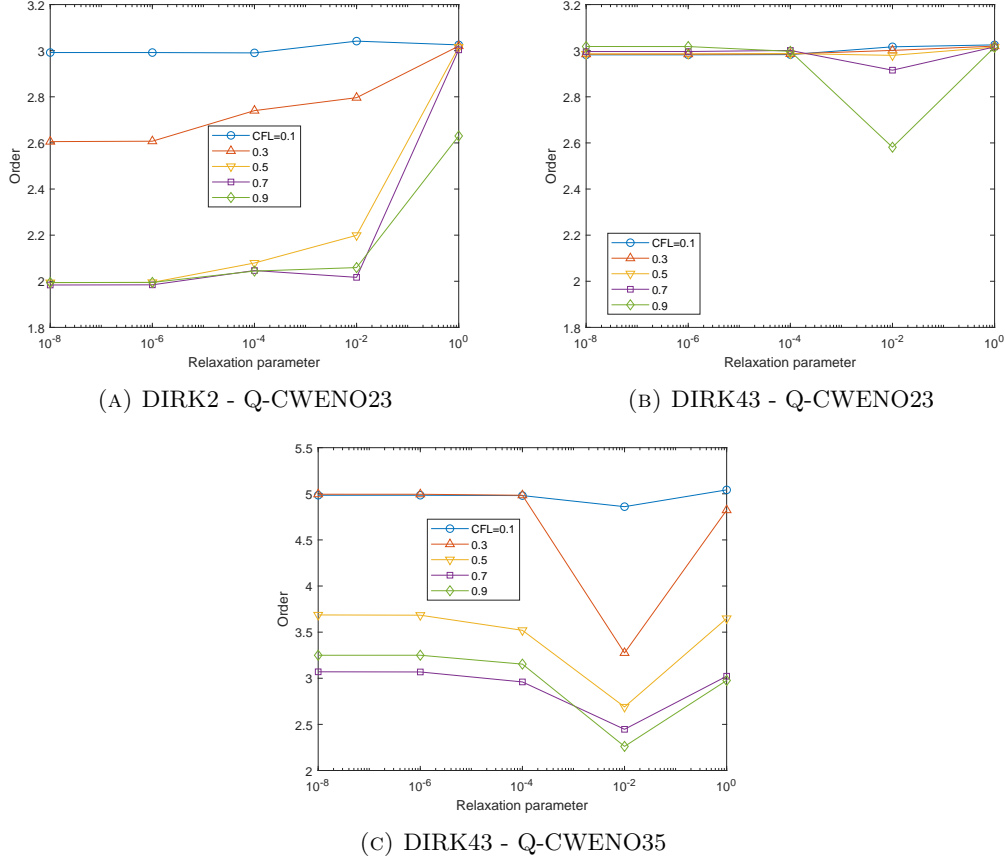


FIGURE 6. Accuracy tests for 1D Xin-Jin model. Initial data is associated to (5.1). x -axis is for the relaxation parameter κ and y -axis is for order of accuracy based on $N_x = 160, 320, 640$.

errors become bigger when we adopt GWENO34 and GWENO46 reconstructions after time $t = 1$, which give wrong shock positions. (See Fig. 7)

- **Discontinuous initial data.** In this test, we again solve the system (4.3) with initial data

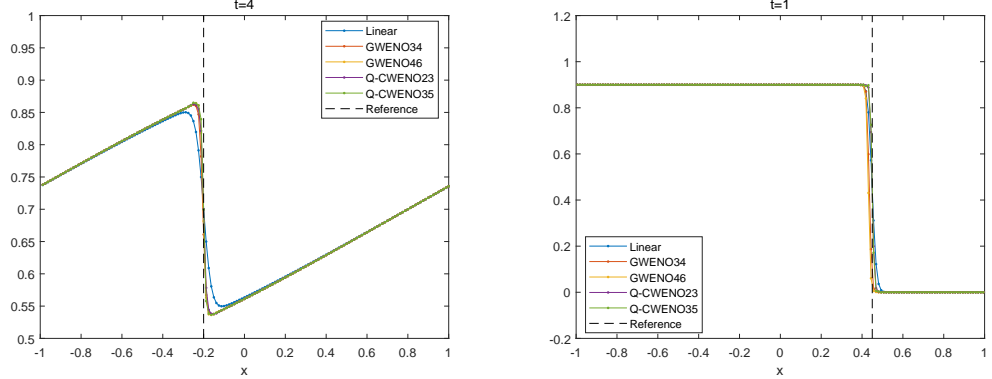
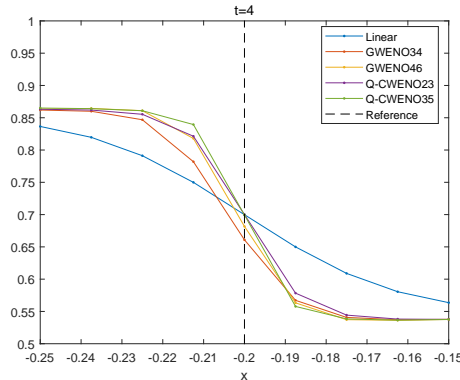
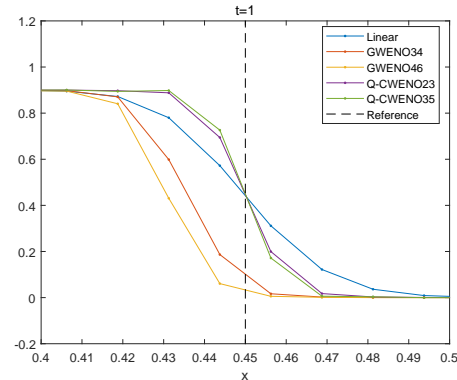
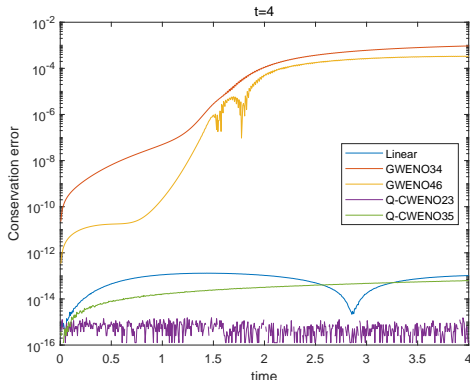
$$(5.3) \quad u_0(x) = \begin{cases} 0.9, & x \leq 0 \\ 0, & x > 0 \end{cases}, \quad v_0(x) = \frac{u_0^2(x)}{2}$$

under freeflow boundary condition on $x \in [-1, 1]$ with grid points $N_x = 160$ up to final time $T^f = 1$. In this test, we compute the conservation error using

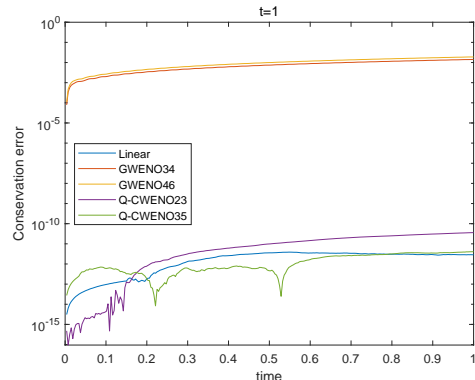
$$E_{con}^n := \frac{\sum_i u_i^n \Delta x - (\sum_i u_i^0 \Delta x + s t^n)}{\sum_i u_i^0 \Delta x},$$

where s is the speed of shock, which is given by $s = 0.45$.

We show our reconstruction can be more effective in capturing shock position. In Fig. 7, we again compare the numerical solutions for different reconstructions. As in the previous shock test, our reconstruction and linear interpolation show better performance in capturing shock position compared to GWENO34 and GWENO46 reconstructions.

(A) Comparison of numerical solutions w.r.t. re-
construction at $x \in [-1, 1]$ (B) Comparison of numerical solutions w.r.t. re-
construction at $x \in [-1, 1]$ (C) Numerical solutions w.r.t. reconstruction at
 $x \in [-0.25, -0.15]$ (D) Numerical solutions w.r.t. reconstruction at
 $x \in [0.4, 0.6]$ 

(E) Conservation errors w.r.t. time



(F) Conservation errors w.r.t. time

FIGURE 7. Shock tests for 1D Xin-Jin model. Left: initial data (5.2) with $\text{CFL} = 0.5$
Right: initial data (5.3) with $\text{CFL} = 0.3$. The results are obtained by DIRK43 based
SL methods for $\kappa = 10^{-8}$ with various reconstructions.

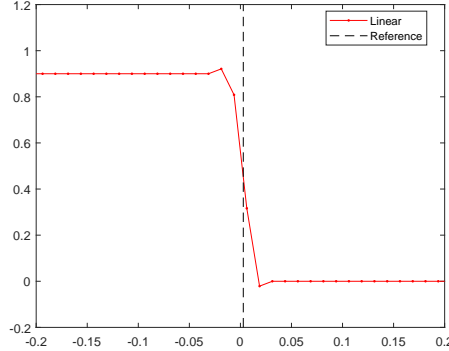


FIGURE 8. Shock test associated to Remark 5.1. For $\kappa = 10^{-8}$, DIRK2 based SL scheme is implemented with linear interpolation. Note that oscillation appears at $T^f = \Delta t = 0.00625$.

Remark 5.1. In the section 5.1, we confirmed that high-order DIRK based SL schemes of Xin-Jin model works for all ranges of relaxation parameters. We also observed that, in the limit $\kappa \rightarrow 0$, oscillations appear near discontinuities for all high-order RK and BDF based SL schemes. To understand this phenomena, as a simple case, consider $F(u) = bu$ for $|b| < 1$. We will show that oscillation appears even after one step $t = t^1$ for arbitrary second order DIRK based SL schemes with linear interpolation (see Fig 8). We use the Butcher's table given by

$$\begin{array}{c|cc} \alpha_1 & \alpha_1 & 0 \\ \hline 1 & 1 - \alpha_2 & \alpha_2 \\ & 1 - \alpha_2 & \alpha_2 \end{array}, \quad \alpha_2 = \frac{\frac{1}{2} - \alpha_1}{1 - \alpha_1}.$$

Then, with the initial conditions (5.3), the following calculation verifies our remark. • Assume $\text{CFL} = \frac{\Delta t}{\Delta x} \leq 1$, and $(u_{i-2}^0, u_{i-1}^0, u_i^0, u_{i+1}^0, u_{i+2}^0) = (0.9, 0.9, 0.9, 0.9, 0)$. Then, in the limit $\kappa \rightarrow 0$, we have

$$\begin{aligned} u_i^1 &= \left(1 - \frac{\Delta t}{\Delta x}\right) u_i^0 + \frac{\Delta t}{2\Delta x} (u_{i-1}^0 + u_{i+1}^0) - \frac{b\Delta t}{2\Delta x} (u_{i-1}^0 - u_{i+1}^0) + \frac{(b^2 - 1)(\Delta t)^2}{8(\Delta x)^2} (u_{i-2}^0 - 2u_i^0 + u_{i+2}^0) \\ &= 0.9 \left(1 + \frac{(1 - b^2)(\Delta t)^2}{8(\Delta x)^2}\right) > 0.9, \end{aligned}$$

for any $\alpha_1 \neq 0, 1$.

5.2. 1D Broadwell model. Now, we move on to the semi-Lagrangian schemes for 1D Broadwell model (4.13).

5.2.1. Accuracy test. To check the accuracy of the proposed schemes, we consider well-prepared data [31]:

$$(5.4) \quad \begin{aligned} \rho_0(x) &= 1 + a_\rho \sin \frac{2\pi}{L} x, & u_0(x) &= \frac{1}{2} + a_u \sin \frac{2\pi}{L} x, \\ z_0(x) &= z_E(\rho_0(x), u_0(x)) + \kappa z_1(\rho_0(x), u_0(x)) \end{aligned}$$

where $a_\rho = 0.3$, $a_u = 0.1$, $L = 20$, $T^f = 30$, and

$$\begin{aligned} z_E(\rho_0, m_0) &= \frac{1}{2\rho_0} (\rho_0^2 + m_0^2), & z_1(\rho_0, m_0) &= -\frac{H(\rho_0, m_0)}{\rho_0}, \\ H(\rho_0, m_0) &= (1 - \partial_\rho z_E + (\partial_m z_E)^2) \partial_x m_0 + (\partial_\rho z_E \partial_m z_E) \partial_x \rho_0. \end{aligned}$$

The periodic condition is imposed on $[-20, 20]$ upto final time $T^f = 30$. We take different CFL numbers less than 1. The order of convergence is based on the grid points $N_x = 160, 320, 640$. Here the desired accuracy for DIRK2 is between 2 and 3, while for DIRK43, it is between 3 and 5.

In Fig. 9, one can see that the DIRK2 based method attains the desired accuracy for all ranges of κ . On the other hand, in the limit $\kappa \rightarrow 0$, the DIRK43 based method shows order reduction, which could be prevented by adopting the BDF3 based method. For small CFL numbers, space errors dominate so the order of accuracy comes from spatial reconstruction, while for large CFL time discretization errors dominate so the order of accuracy comes from time integration.

5.3. Shock tests. We consider the following two cases in [4]:

$$(5.5) \quad \begin{aligned} \text{Case 1. } (\rho, m, z) &= \begin{cases} (2, 1, 1) & x < 0.2 \\ (1, 0.13962, 1) & x > 0.2 \end{cases}, x \in [-1, 1], T^f = 0.25, \kappa = 1, \\ \text{Case 2. } (\rho, m, z) &= \begin{cases} (1, 0, 1) & x < 0.5 \\ (0.2, 0, 1) & x > 0.5 \end{cases}, x \in [0, 1], T^f = 0.25, \kappa = 10^{-8}. \end{aligned}$$

For each case, we take $N_x = 200$. In Fig. 10 we observe that the proposed schemes allows large $\text{CFL} > 1$ with the choice of $\kappa = 1$. In case of $\kappa = 10^{-8}$, some oscillations appear near the discontinuity for $\text{CFL} > 0.8$. For $\text{CFL} \leq 0.8$, we obtain solutions which reproduce the numerical results in [4].

5.4. 2D simplified Xin-Jin model. For 2D tests, we here consider the DIRK2 based method.

5.4.1. Accuracy test. Here, we use well-prepared initial data:

$$(5.6) \quad u_0(x, y) = 0.8 \sin^2(\pi x) \sin^2(\pi y), \quad v_0(x, y) = \frac{u_0^2(x, y)}{2} + \kappa (u_0^2(x, y) - 1) (\partial_x u_0(x, y) + \partial_y u_0(x, y)).$$

The computation is performed in $(x, y) \in [0, 1]^2$ with the periodic boundary condition with $N_x = N_y$. In this problem, the breaking time is $T_b = \frac{1}{0.6\pi\sqrt{3}} \approx 0.3063$, we take a final time as $T^f = 0.15$. Since $|u_0| < 1$, the subcharacteristic condition is satisfied. We restrict the ratio to satisfy $\frac{\Delta t}{\Delta x} \leq 1$. In Fig. 11, we confirm that SL schemes based on DIRK2 and BDF2 attains desired accuracy between 2 and 3 for all ranges of the relaxation parameter κ .

5.4.2. Shock tests. Now, we move on to 2D shock tests for (4.3).

• **Smooth initial data.** Here, we solve the relaxation system (4.3) to capture the profile of the shock in Burgers equation. For this, we consider the following initial data:

$$(5.7) \quad u_0(x, y) = 0.8 \sin^2(\pi x) \sin^2(\pi y), \quad v_0(x, y) = \frac{u_0^2(x, y)}{2}.$$

on the periodic domain $(x, y) \in [0, 1]^2$ with grid points $N_x = 400$ and mesh ratio $\frac{\Delta t}{\Delta x} = \frac{\Delta t}{\Delta y} = 0.2$. In Fig. 12, results are reported for $t = 1, 2, 3$. Here, we only present result using 2D SL methods based on DIRK2 and Q-CWENO23.

• **Discontinuous initial data.** This test has been solved by solving a viscous Burgers equation in [15]. Here, we instead solve the relaxation system (4.3) to capture the correct shock position of Burgers equation. Initial data is given by

$$(5.8) \quad u_0(x) = \begin{cases} -0.5, & x \leq 0, y \leq 0 \\ 0.25, & x \leq 0, y > 0 \\ 0.25, & x > 0, y \leq 0 \\ 0.5, & x > 0, y > 0 \end{cases}, \quad v_0(x, y) = \frac{u_0^2(x, y)}{2}$$

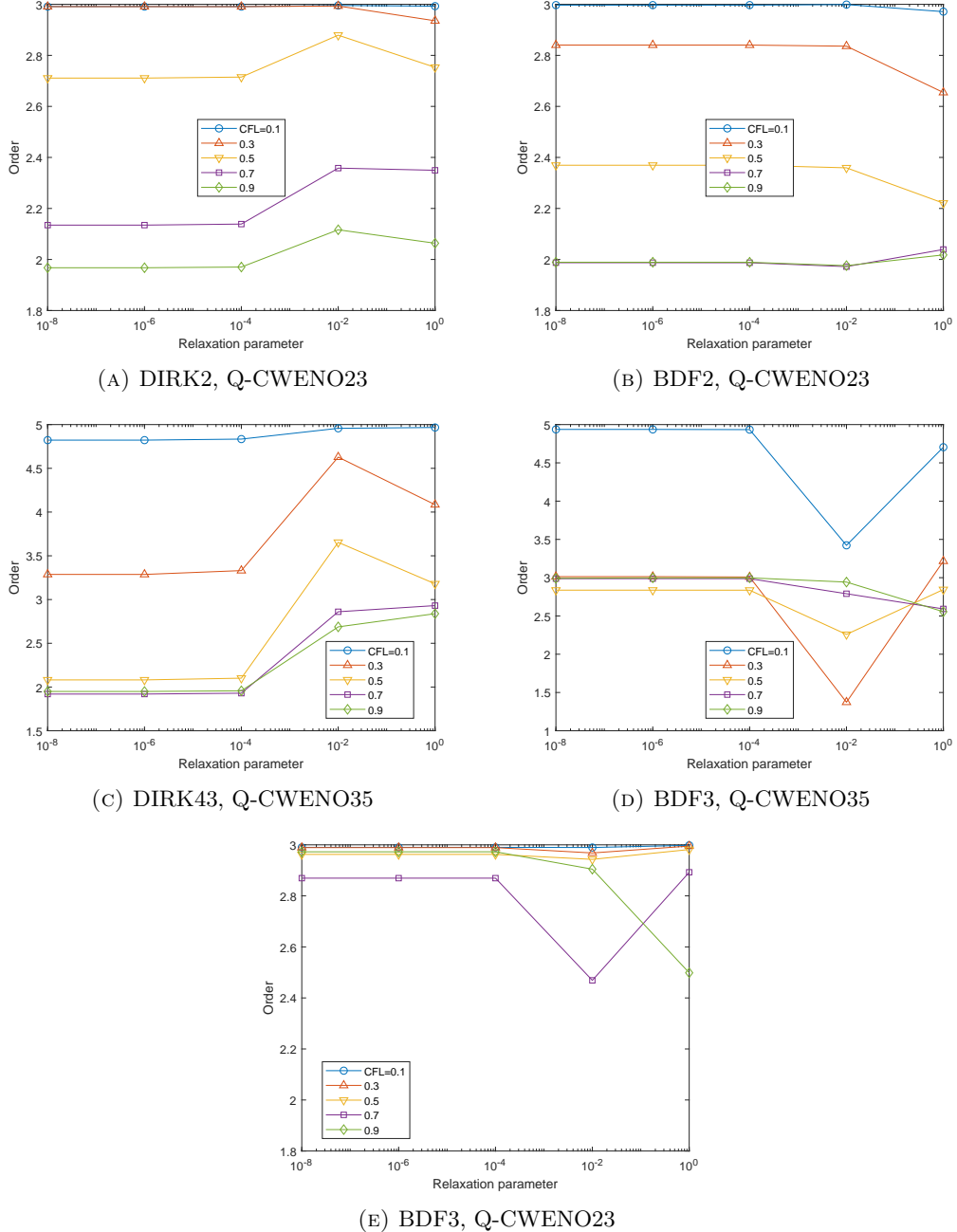
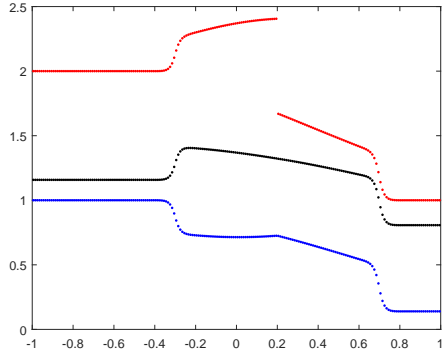
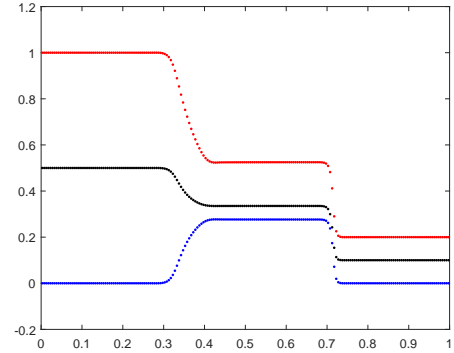


FIGURE 9. Accuracy tests for 1D Broadwell model. Initial data is associated to (5.4). x -axis is for the relaxation parameter κ and y -axis is for order of accuracy based on $N_x = 160, 320, 640$.

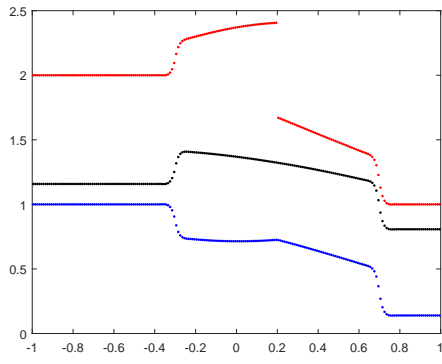
with freeflow boundary condition $(x, y) \in [-1, 1]^2$ with grid points $N_x = 400$ and mesh ratio $\frac{\Delta t}{\Delta x} = \frac{\Delta t}{\Delta y} = 0.2$. In Fig. 13, we plot the results for $t = 1, 2, 3$. We only present result using 2D SL methods based on DIRK2 and Q-CWENO23.



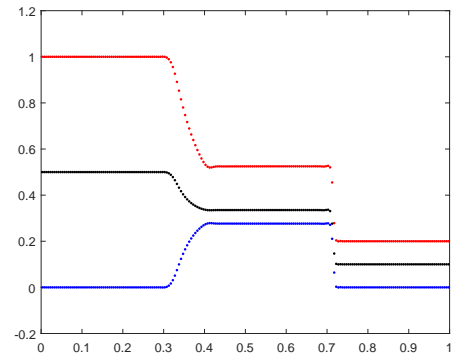
(A) DIRK2, Q-CWENO23, CFL = 0.5



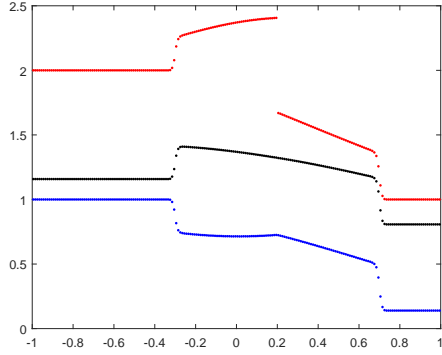
(B) DIRK2, Q-CWENO23, CFL = 0.5



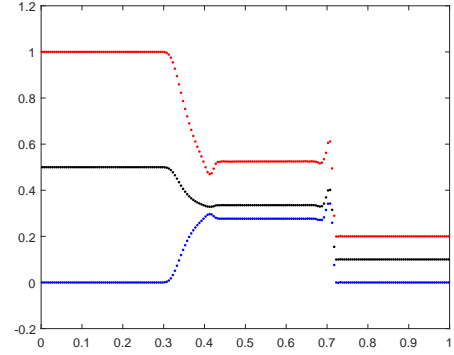
(C) DIRK2, Q-CWENO23, CFL = 0.8



(D) DIRK2, Q-CWENO23, CFL = 0.8



(E) DIRK2, Q-CWENO23, CFL = 1.9



(F) DIRK2, Q-CWENO23, CFL = 1.9

FIGURE 10. Shock tests for 1D Broadwell model. Macroscopic variables ρ (red), m (blue) and z (black). Left: Case 1 in (5.5), Right: Case 2 in (5.5).

6. CONCLUSIONS

We propose a simple technique to restore conservation in semi-Lagrangian schemes when non-linear reconstructions are adopted to avoid spurious oscillation or to preserve the positivity of the solution. The reconstruction is obtained by taking the sliding average of a basic non-oscillatory (positive-preserving) cell-average to point-wise reconstruction R , thus it inherits the non-oscillatory

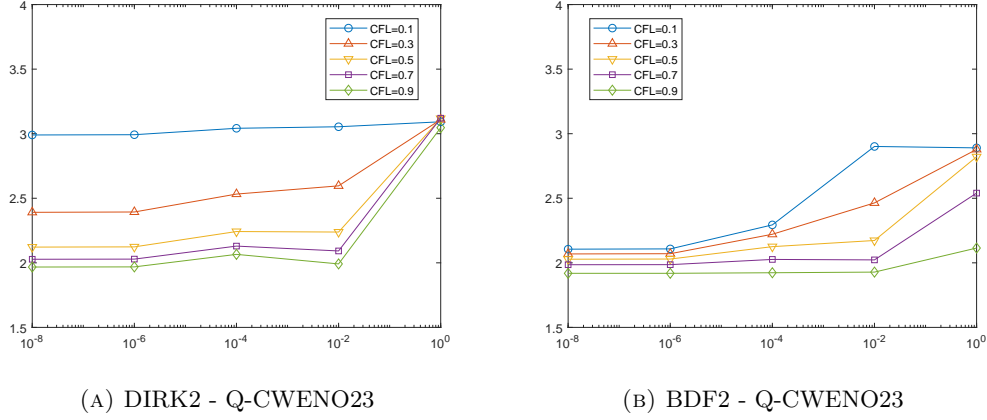


FIGURE 11. Accuracy tests for 2D Xin-Jin model. Initial data is associated to (5.6). x -axis is for the relaxation parameter κ and y -axis is for order of accuracy based on $N_x^2 = N_y^2 = 160^2, 320^2, 640^2$.

(positivity-preserving) property of R . A detailed analysis is performed of the proposed reconstruction, proving its accuracy and conservation properties, and its consistency with Lagrange interpolation in the case of linear basic reconstruction. Two dimensional extension is also considered and analyzed. The technique is then tested on the Xin-Jin relaxation system in one and two space dimensions, and on the 1D Broadwell model. Applications to BGK model and Vlasov-Poisson system will be presented in the second part of the paper.

APPENDIX A. PROOF OF PROPOSITION 2.1

Proof. We first write (2.7) as

$$(A.1) \quad Q_{i+\theta} = \sum_{\ell=\text{even}}^k (\Delta x)^\ell \left(\alpha_\ell(\theta) R_i^{(\ell)} + \left(\frac{1}{(\ell+1)!} \left(\frac{1}{2} \right)^\ell - \alpha_\ell(\theta) \right) R_{i+1}^{(\ell)} \right) + \sum_{\ell=\text{odd}}^k (\Delta x)^\ell \alpha_\ell(\theta) (R_i^{(\ell)} - R_{i+1}^{(\ell)}).$$

This, together with the assumption (2.12), gives

$$\begin{aligned} Q_{i+\theta} &= \sum_{\ell=\text{even}}^k (\Delta x)^\ell \left(\alpha_\ell(\theta) u_i^{(\ell)} + \left(\frac{1}{(\ell+1)!} \left(\frac{1}{2} \right)^\ell - \alpha_\ell(\theta) \right) u_{i+1}^{(\ell)} \right) \\ &\quad + \sum_{\ell=\text{odd}}^k (\Delta x)^\ell \alpha_\ell(\theta) (u_i^{(\ell)} - u_{i+1}^{(\ell)}) + (\Delta x)^{k+2} \\ &= \sum_{\ell=0}^k (\Delta x)^\ell \left(\alpha_\ell(\theta) u_i^{(\ell)} + \beta_\ell(\theta) u_{i+1}^{(\ell)} \right) + (\Delta x)^{k+2}. \end{aligned}$$

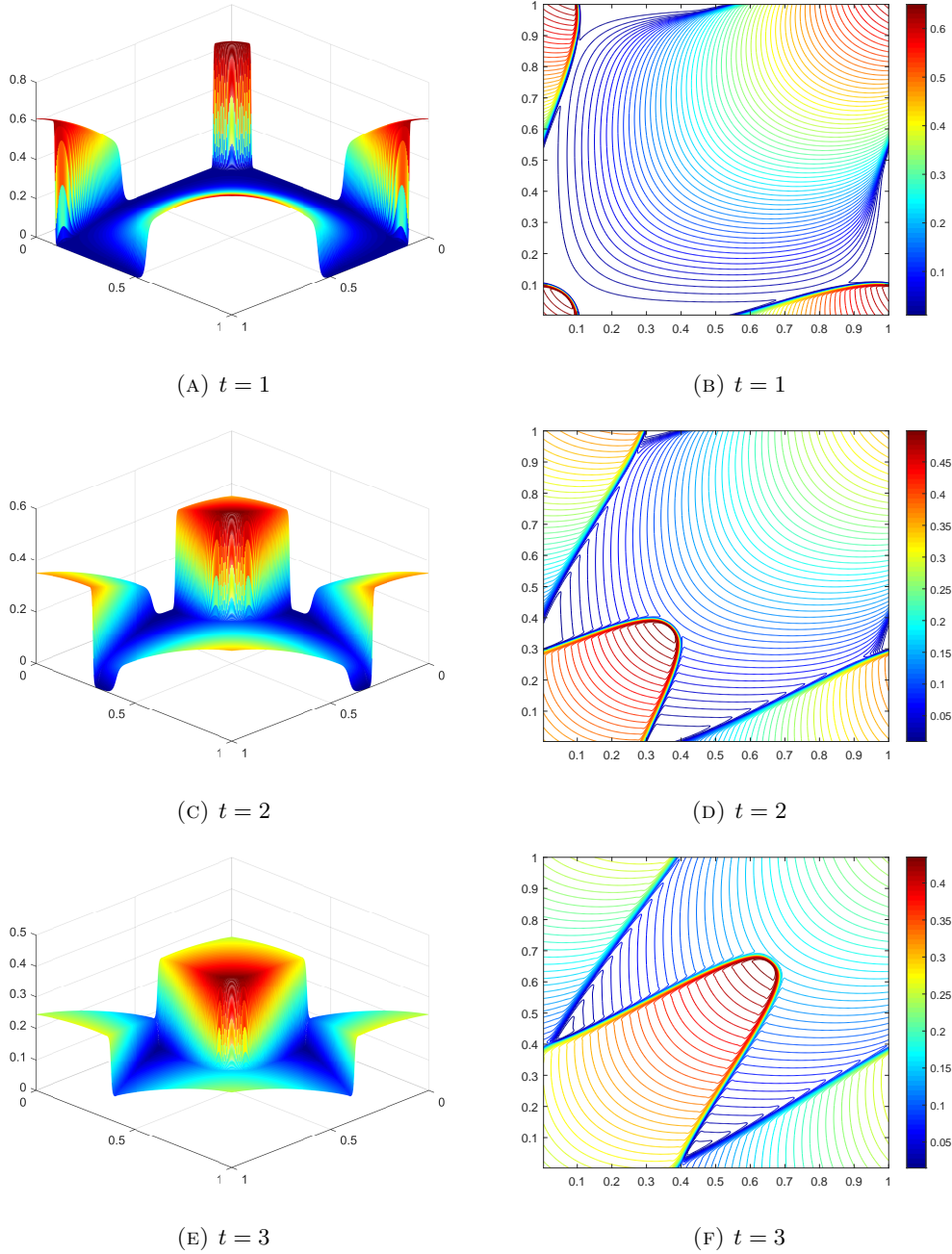


FIGURE 12. Shock test for 2D Xin-Jin model. Initial data is associated to (5.7). Numerical solutions are obtained by DIRK2 based SL scheme for $\kappa = 10^{-4}$. Mesh plot (left) and contour plot (right) of the solution u at various times $t = 1, 2, 3$.

Using Taylor's expansion $u_{i+1}^{(\ell)} = u_i^{(\ell)} + u_i^{(\ell+1)}\Delta x + \frac{1}{2}u_i^{(\ell+2)}(\Delta x)^2 + \frac{1}{6}u_i^{(\ell+3)}(\Delta x)^3 + \dots$, we obtain

$$\begin{aligned}
 Q_{i+\theta} &= \sum_{\ell=0}^k (\Delta x)^\ell \left(\alpha_\ell(\theta)u_i^{(\ell)} + \beta_\ell(\theta) \sum_{m=0}^{k+1-\ell} \frac{u_i^{(\ell+m)}}{m!}(\Delta x)^m \right) + \mathcal{O}((\Delta x)^{k+2}) \\
 &= \sum_{\ell=0}^k (\Delta x)^\ell \alpha_\ell(\theta)u_i^{(\ell)} + \sum_{\ell=0}^k \sum_{m=0}^{k-\ell} (\Delta x)^{\ell+m} \beta_\ell(\theta) \frac{u_i^{(\ell+m)}}{m!} + \sum_{\ell=0}^k (\Delta x)^{k+1} \beta_\ell(\theta) \frac{u_i^{(k+1)}}{(k+1-\ell)!} + \mathcal{O}((\Delta x)^{k+2}) \\
 &=: \sum_{\ell=0}^k (\Delta x)^\ell \lambda_\ell(\theta)u_i^{(\ell)} + \sum_{\ell=0}^k (\Delta x)^{k+1} \beta_\ell(\theta) \frac{u_i^{(k+1)}}{(k+1-\ell)!} + \mathcal{O}((\Delta x)^{k+2}),
 \end{aligned}$$

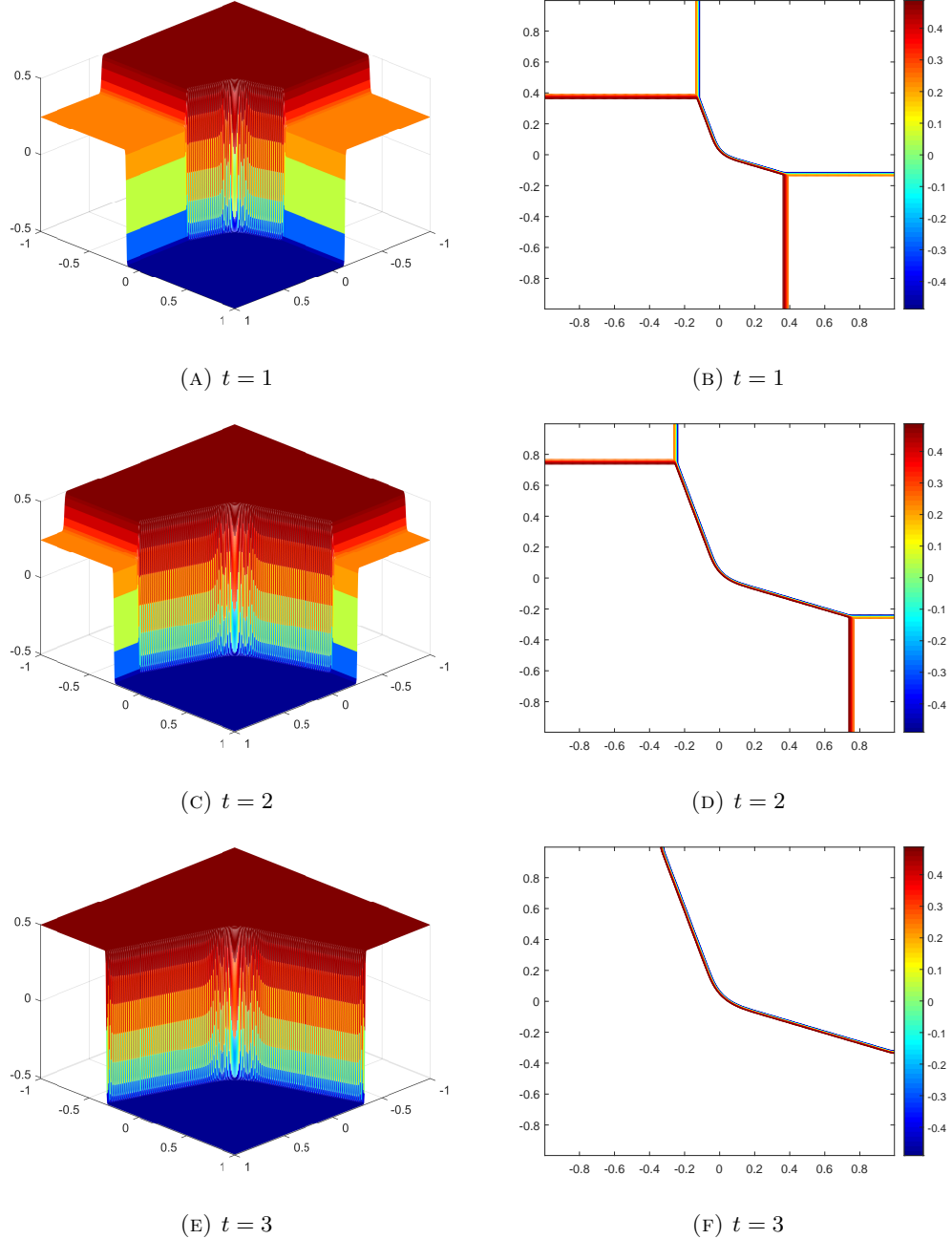


FIGURE 13. Shock test for 2D Xin-Jin model. Initial data is associated to (5.8). Numerical solutions are obtained by DIRK2 based SL scheme for $\kappa = 10^{-4}$. Mesh plot (left) and contour plot (right) of the solution u at various times $t = 1, 2, 3$.

where $\lambda_\ell(\theta) = \alpha_\ell(\theta) + \sum_{m=0}^{\ell} \beta_m(\theta) \frac{1}{(\ell-m)!}$. Note that

$$\sum_{\ell=0}^k \beta_\ell(\theta) \frac{1}{(k+1-\ell)!} = \alpha_{k+1}(\theta) + \sum_{m=0}^{k+1} \beta_m(\theta) \frac{1}{(k+1-m)!} = \lambda_{k+1}(\theta).$$

The first equality follows from $\alpha_{k+1}(\theta) + \beta_{k+1}(\theta) = 0$, which holds due to (2.9) for an even integer k . To sum up,

$$Q_{i+\theta} = \sum_{\ell=0}^{k+1} (\Delta x)^\ell \lambda_\ell(\theta) u_i^{(\ell)} + \mathcal{O}((\Delta x)^{k+2}),$$

and this can be written explicitly as follows:

$$\begin{aligned} Q_{i+\theta} &= u_i^{(0)} + \theta u_i^{(1)} \Delta x + \left(\frac{\theta^2}{2} + \frac{1}{24} \right) u_i^{(2)} (\Delta x)^2 + \left(\frac{\theta^3}{6} + \frac{\theta}{24} \right) u_i^{(3)} (\Delta x)^3 \\ &\quad + \left(\frac{\theta^4}{24} + \frac{\theta^2}{48} + \frac{1}{1920} \right) u_i^{(4)} (\Delta x)^4 + \left(\frac{\theta^5}{120} + \frac{\theta^3}{144} + \frac{\theta}{1920} \right) u_i^{(5)} (\Delta x)^5 \\ &\quad + \left(\frac{\theta^6}{720} + \frac{\theta^4}{576} + \frac{\theta^2}{3840} + \frac{1}{322560} \right) u_i^{(6)} (\Delta x)^6 + \cdots + \mathcal{O}((\Delta x)^{k+2}) \\ &= \sum_{\ell=0}^{k+1} \frac{\theta^\ell}{\ell!} u_i^{(\ell)} (\Delta x)^\ell + \frac{(\Delta x)^2}{24} \sum_{\ell=0}^{k-1} \frac{\theta^\ell}{\ell!} u_i^{(\ell+2)} (\Delta x)^\ell + \frac{(\Delta x)^4}{1920} \sum_{\ell=0}^{k-3} \frac{\theta^\ell}{\ell!} u_i^{(\ell+4)} (\Delta x)^\ell \\ &\quad + \frac{(\Delta x)^6}{322560} \sum_{\ell=0}^{k-5} \frac{\theta^\ell}{\ell!} u_i^{(\ell+4)} (\Delta x)^\ell + \cdots + \mathcal{O}((\Delta x)^{k+2}). \end{aligned}$$

Consequently, we can derive

$$\begin{aligned} Q_{i+\theta} &= u(x_{i+\theta}) + \frac{(\Delta x)^2}{24} u^{(2)}(x_{i+\theta}) + \frac{(\Delta x)^4}{1920} u^{(4)}(x_{i+\theta}) + \cdots + \mathcal{O}((\Delta x)^{k+2}) \\ &= \sum_{\ell=\text{even}}^k (\Delta x)^\ell u^{(\ell)}(x_{i+\theta}) \frac{1}{(\ell+1)!} \left(\frac{1}{2} \right)^\ell + \mathcal{O}((\Delta x)^{k+2}) \\ &= \bar{u}(x_{i+\theta}) + \mathcal{O}((\Delta x)^{k+2}). \end{aligned}$$

□

APPENDIX B. PROOF OF REMARK 2.1

Consider any polynomial reconstruction $R_i(x), R_{i+1}(x) \in \mathbb{P}^k$ of the form (2.4) such that

$$u^{(\ell)}(x_i) - R_i^{(\ell)} = \mathcal{O}((\Delta x)^{k+1-\ell}), \quad u^{(\ell)}(x_{i+1}) - R_{i+1}^{(\ell)} = \mathcal{O}((\Delta x)^{k+1-\ell}).$$

From the assumption that $R_i^{(\ell)}$ is represented by Lipschitz functions F_ℓ of $\{\bar{u}_{i-r}, \dots, \bar{u}_{i+s}\}$, we can write it as

$$R_i^{(\ell)} = u^{(\ell)}(x_i) + F_\ell(\bar{u}_{i-r}, \dots, \bar{u}_{i+s}) - u^{(\ell)}(x_i),$$

where $F_\ell(\bar{u}_{i-r}, \dots, \bar{u}_{i+s}) - u^{(\ell)}(x_i) = \mathcal{O}((\Delta x)^{k+1-\ell})$. Also, in (2.13), one can see that the function $p_i^{(\ell)} \in \mathbb{P}^{k-\ell}$ is written with a Lipschitz function G_ℓ of $\{\bar{u}_{i-r}, \dots, \bar{u}_{i+s}\}$ such that

$$p_i^{(\ell)} = u^{(\ell)}(x_i) + G_\ell(\bar{u}_{i-r}, \dots, \bar{u}_{i+s}) - u^{(\ell)}(x_i), \quad G_\ell(\bar{u}_{i-r}, \dots, \bar{u}_{i+s}) - u^{(\ell)}(x_i) = \mathcal{O}((\Delta x)^{k+1-\ell}).$$

Now, let us define $H_\ell(\{\bar{u}_{i-r}, \dots, \bar{u}_{i+s}\})$ by

$$H_\ell(\bar{u}_{i-r}, \dots, \bar{u}_{i+s}) := G_\ell(\bar{u}_{i-r}, \dots, \bar{u}_{i+s}) - F_\ell(\bar{u}_{i-r}, \dots, \bar{u}_{i+s}),$$

then it is Lipschitz continuous w.r.t. $\{\bar{u}_{i-r}, \dots, \bar{u}_{i+s}\}$ and $H^\ell(\bar{u}_{i-r}, \dots, \bar{u}_{i+s}) = \mathcal{O}((\Delta x)^{k+1-\ell})$. Consequently,

$$\begin{aligned} u^{(\ell)}(x_i) - R_i^{(\ell)} &= \left(u^{(\ell)}(x_{i+1}) - R_{i+1}^{(\ell)} \right) \\ &= \left\{ u^{(\ell)}(x_i) - p_i^{(\ell)} - \left(u^{(\ell)}(x_{i+1}) - p_{i+1}^{(\ell)} \right) \right\} + \left(p_i^{(\ell)} - R_i^{(\ell)} \right) - \left(p_{i+1}^{(\ell)} - R_{i+1}^{(\ell)} \right) \\ &= \mathcal{O}((\Delta x)^{k+2-\ell}) + H_\ell(\{\bar{u}_{i-r}, \dots, \bar{u}_{i+s}\}) - H_\ell(\{\bar{u}_{i+1-r}, \dots, \bar{u}_{i+1+s}\}) \\ &= \mathcal{O}((\Delta x)^{k+2-\ell}). \end{aligned}$$

APPENDIX C. PROOF OF PROPOSITION 2.2

Proof. The proof is divided into three steps

Step 1, Reconstruction of $R_i(x)$: This polynomial reconstruction is also introduced in [35]. Given cell average values $\{\bar{u}_i\}$, we first consider a primitive function $U(x) := \int_{-\infty}^x u(x)dx$ and compute its cell boundary values as

$$U(x_{i+j-\frac{1}{2}}) = \int_{-\infty}^{x_{i+j-\frac{1}{2}}} u(x) dx = \sum_{m=-\infty}^{i+j-1} \bar{u}_m \Delta x, \quad -r \leq j \leq r+1.$$

Then, look for a polynomial $P_i(x)$ such that

$$P_i(x_{i+j-\frac{1}{2}}) = U(x_{i+j-\frac{1}{2}}), \quad -r \leq j \leq r+1.$$

By differentiating $P_i(x)$, we obtain the basic reconstruction $R_i(x)$ which satisfies

$$P'_i(x) = R_i(x) = u(x) + \mathcal{O}((\Delta x)^{k+1})$$

and the condition (2.14). The resulting form of $R_i(x)$ is given by

$$R_i(x) = \sum_{m=1}^{k+1} \sum_{j=0}^{m-1} \bar{u}_{i-r+j} \Delta x \left\{ \frac{\sum_{\ell=0, \ell \neq m}^{k+1} \prod_{q=0, q \neq m, \ell}^{k+1} (x - x_{i-r+\ell-\frac{1}{2}})}{\prod_{\ell=0, \ell \neq m}^{k+1} (x_{i-r+m-\frac{1}{2}} - x_{i-r+\ell-\frac{1}{2}})} \right\}.$$

Step 2, Reconstruction of $Q_{i+\theta}$: To reconstruct $Q_{i+\theta}$, we first compute the cell average value of $R_i(x)$ on $[x_{i-\frac{1}{2}+\theta}, x_{i+\frac{1}{2}}]$:

$$(C.1) \quad \frac{1}{\Delta x} \int_{x_{i-\frac{1}{2}+\theta}}^{x_{i+\frac{1}{2}}} R_i(x) dx = \sum_{m=1}^{k+1} \sum_{j=0}^{m-1} \bar{u}_{i-r+j} \left\{ \frac{\prod_{\ell=0, \ell \neq m}^{k+1} (r - \ell + 1) - \prod_{\ell=0, \ell \neq m}^{k+1} (\theta + r - \ell)}{\prod_{\ell=0, \ell \neq m}^{k+1} (m - \ell)} \right\},$$

which directly come from

$$\int_{x_{i-\frac{1}{2}+\theta}}^{x_{i+\frac{1}{2}}} \left(\sum_{\ell=0, \ell \neq m}^{k+1} \prod_{q=0, q \neq m, \ell}^{k+1} (x - x_{i-r+\ell-\frac{1}{2}}) \right) dx = \prod_{\ell=0, \ell \neq m}^{k+1} x_{r-\ell+1} - \prod_{\ell=0, \ell \neq m}^{k+1} x_{\theta+r-\ell}.$$

Similarly, we compute the cell average of $R_{i+1}(x)$ on $[x_{i+\frac{1}{2}}, x_{i+\frac{1}{2}+\theta}]$:

$$(C.2) \quad \frac{1}{\Delta x} \int_{x_{i+\frac{1}{2}}}^{x_{i+\frac{1}{2}+\theta}} R_{i+1}(x) dx = \sum_{m=1}^{k+1} \sum_{j=1}^m \bar{u}_{i-r+j} \left\{ \frac{\prod_{\ell=0, \ell \neq m}^{k+1} (\theta + r - \ell) - \prod_{\ell=0, \ell \neq m}^{k+1} (r - \ell)}{\prod_{\ell=0, \ell \neq m}^{k+1} (m - \ell)} \right\}.$$

Now, we insert (C.1) and (C.2) into the identity for $Q_{i+\theta}$ in (2.3):

$$Q_{i+\theta} = \frac{1}{\Delta x} \int_{x_{i-\frac{1}{2}+\theta}}^{x_{i+\frac{1}{2}}} R_i(x) dx + \frac{1}{\Delta x} \int_{x_{i+\frac{1}{2}}}^{x_{i+\frac{1}{2}+\theta}} R_{i+1}(x) dx,$$

and decompose this into four parts:

$$\begin{aligned}
Q_{i+\theta} &= \sum_{j=0} \sum_{m=j+1}^{k+1} \bar{u}_{i-r+j} \left\{ \frac{\prod_{\ell=0, \ell \neq m}^{k+1} (r - \ell + 1) - \prod_{\ell=0, \ell \neq m}^{k+1} (\theta + r - \ell)}{\prod_{\ell=0, \ell \neq m}^{k+1} (m - \ell)} \right\} \\
&\quad + \sum_{j=k+1} \sum_{m=j}^{k+1} \bar{u}_{i-r+j} \left\{ \frac{\prod_{\ell=0, \ell \neq m}^{k+1} (\theta + r - \ell) - \prod_{\ell=0, \ell \neq m}^{k+1} (r - \ell)}{\prod_{\ell=0, \ell \neq m}^{k+1} (m - \ell)} \right\} \\
&\quad + \sum_{j=1}^k \sum_{m=j}^{k+1} \bar{u}_{i-r+j} \left\{ \frac{\prod_{\ell=0, \ell \neq m}^{k+1} (\theta + r - \ell) - \prod_{\ell=0, \ell \neq m}^{k+1} (r - \ell)}{\prod_{\ell=0, \ell \neq m}^{k+1} (m - \ell)} \right\} \\
&\quad + \sum_{j=1}^k \sum_{m=j+1}^{k+1} \bar{u}_{i-r+j} \left\{ \frac{\prod_{\ell=0, \ell \neq m}^{k+1} (r - \ell + 1) - \prod_{\ell=0, \ell \neq m}^{k+1} (r - \ell)}{\prod_{\ell=0, \ell \neq m}^{k+1} (m - \ell)} \right\} \\
&=: I_1 + I_2 + I_3 + I_4.
\end{aligned}$$

With the identity $\sum_{m=0}^{k+1} \frac{\prod_{\ell=0, \ell \neq m}^{k+1} (\theta + r - \ell)}{\prod_{\ell=0, \ell \neq m}^{k+1} (m - \ell)} = 1$, we can simplify I_1 as

$$\begin{aligned}
(C.3) \quad I_1 &= \bar{u}_{i-r} \sum_{m=1}^{k+1} \left\{ \frac{\prod_{\ell=0, \ell \neq m}^{k+1} (r - \ell + 1) - \prod_{\ell=0, \ell \neq m}^{k+1} (\theta + r - \ell)}{\prod_{\ell=0, \ell \neq m}^{k+1} (m - \ell)} \right\} \\
&= \bar{u}_{i-r} \left(\sum_{m=r+1} \frac{\prod_{\ell=0, \ell \neq m}^{k+1} (r - \ell + 1)}{\prod_{\ell=0, \ell \neq m}^{k+1} (m - \ell)} - \sum_{m=1}^{k+1} \frac{\prod_{\ell=0, \ell \neq m}^{k+1} (\theta + r - \ell)}{\prod_{\ell=0, \ell \neq m}^{k+1} (m - \ell)} \right) \\
&= \bar{u}_{i-r} \left(1 - \sum_{m=1}^{k+1} \frac{\prod_{\ell=0, \ell \neq m}^{k+1} (\theta + r - \ell)}{\prod_{\ell=0, \ell \neq m}^{k+1} (m - \ell)} \right) \\
&= \bar{u}_{i-r} \frac{\prod_{\ell=1}^{k+1} (\theta + r - \ell)}{\prod_{\ell=1}^{k+1} (-\ell)}.
\end{aligned}$$

The I_2 and I_3 terms are calculated as

$$\begin{aligned}
(C.4) \quad I_2 &= \bar{u}_{i+r+1} \left\{ \frac{\prod_{\ell=0}^k (\theta + r - \ell) - \prod_{\ell=0}^k (r - \ell)}{\prod_{\ell=0}^k (k + 1 - \ell)} \right\} = \bar{u}_{i+r+1} \frac{\prod_{\ell=0}^k \theta + r - \ell}{\prod_{\ell=0}^k k + 1 - \ell} \\
I_3 &= \sum_{j=1}^k \bar{u}_{i-r+j} \left\{ \frac{\prod_{\ell=0, \ell \neq j}^{k+1} (\theta + r - \ell) - \prod_{\ell=0, \ell \neq j}^{k+1} (r - \ell)}{\prod_{\ell=0, \ell \neq j}^{k+1} (j - \ell)} \right\} \\
&= \bar{u}_i \left(\frac{\prod_{\ell=0, \ell \neq r}^{k+1} (\theta + r - \ell)}{\prod_{\ell=0, \ell \neq r}^{k+1} (r - \ell)} - 1 \right) + \sum_{j=1, j \neq r}^k \bar{u}_{i-r+j} \left\{ \frac{\prod_{\ell=0, \ell \neq j}^{k+1} \theta + r - \ell}{\prod_{\ell=0, \ell \neq j}^{k+1} j - \ell} \right\}.
\end{aligned}$$

A direct computation leads to $I_4 = \bar{u}_i$. This, combined with (C.3), (C.4), gives

$$(C.5) \quad Q_{i+\theta} = \sum_{j=0}^{k+1} \bar{u}_{i-r+j} \prod_{\ell=0, \ell \neq j}^{k+1} \frac{\theta + r - \ell}{j - \ell}.$$

Step 3, Comparison of $Q_{i+\theta}$ and $L(x_{i+\theta})$: For the comparison, we consider a Lagrange polynomial $L(x)$ which satisfies $L(x_{i-r+j}) = \bar{u}_{i-r+j}$ for $0 \leq j \leq k+1$:

$$L(x) = \sum_{j=0}^{k+1} \bar{u}_{i-r+j} \prod_{\ell=0, \ell \neq j}^{k+1} \frac{x - x_{i-r+\ell}}{x_{i-r+j} - x_{i-r+\ell}}.$$

Inserting $x = x_{i+\theta}$ into $L(x)$, we obtain $L(x_{i+\theta}) = Q_{i+\theta}$. This completes the proof. \square

APPENDIX D. PROOF THAT THE CONDITION (2.12) IN PROPOSITION 2.1 IS SATISFIED BY BOTH CWENO23 AND CWENO23Z.

Here, we check if the condition (2.12) is satisfied by (2.19). For this, we assume that u is smooth enough so that $\omega_C^i = \frac{1}{2} + e_C^i$ for $e_C^i = \mathcal{O}((\Delta x)^2)$. We refer to [26] for the assumption. Then, we have

$$\begin{aligned} R_i^{(0)} &= \bar{u}_i - \frac{1}{12} \left(C_C + e_C^i \right) (\bar{u}_{i+1} - 2\bar{u}_i + \bar{u}_{i-1}) \\ (D.1) \quad &= \bar{u}_i - \frac{1}{12} \left(\frac{1}{2} + \mathcal{O}((\Delta x)^2) \right) ((\Delta x)^2 \bar{u}_i'' + \mathcal{O}((\Delta x)^4)) \\ &= \bar{u}_i - \frac{1}{24} ((\Delta x)^2 \bar{u}_i'') + \mathcal{O}((\Delta x)^4) \\ &= u_i + \mathcal{O}((\Delta x)^4). \end{aligned}$$

Similarly, we write $\omega_L^i = \frac{1}{4} + e_L^i$ and $\omega_R^i = \frac{1}{4} + e_R^i$ with $e_L^i, e_R^i = \mathcal{O}((\Delta x)^2)$. Then,

$$\begin{aligned} R_i^{(1)} &= \omega_L^i \frac{\bar{u}_i - \bar{u}_{i-1}}{\Delta x} + \omega_R^i \frac{\bar{u}_{i+1} - \bar{u}_i}{\Delta x} + \omega_C^i \frac{\bar{u}_{i+1} - \bar{u}_{i-1}}{2\Delta x} \\ &= \left(\frac{1}{4} + e_L^i \right) \left[\bar{u}'_i - \frac{\Delta x}{2} \bar{u}''_i + \frac{(\Delta x)^2}{6} \bar{u}'''_i \right] + \left(\frac{1}{4} + e_R^i \right) \left[\bar{u}'_i + \frac{\Delta x}{2} \bar{u}''_i + \frac{(\Delta x)^2}{6} \bar{u}'''_i \right] \\ &\quad + \left(\frac{1}{2} + e_C^i \right) \left[\bar{u}'_i + \frac{1}{6} (\Delta x)^2 \bar{u}'''_i \right] + \mathcal{O}((\Delta x)^3) \\ &= \bar{u}'_i + \frac{(\Delta x)^2}{6} \bar{u}'''_i + \mathcal{O}((\Delta x)^3). \end{aligned}$$

In the last equality, we used $\sum_k \omega_k^i = 1$. Hence, we can obtain

$$\begin{aligned} (D.2) \quad R_i^{(1)} - R_{i+1}^{(1)} &= \bar{u}'_i - \bar{u}'_{i+1} + \frac{(\Delta x)^2}{6} (\bar{u}'''_i - \bar{u}'''_{i+1}) + \mathcal{O}((\Delta x)^3) \\ &= \bar{u}'_i - \bar{u}'_{i+1} - \frac{(\Delta x)^2}{24} (\bar{u}'''_i - \bar{u}'''_{i+1}) + \mathcal{O}((\Delta x)^3) \\ &= \left(\bar{u}'_i - \frac{(\Delta x)^2}{24} \bar{u}'''_i \right) - \left(\bar{u}'_{i+1} - \frac{(\Delta x)^2}{24} \bar{u}'''_{i+1} \right) + \mathcal{O}((\Delta x)^3) = u'_i - u'_{i+1} + \mathcal{O}((\Delta x)^3). \end{aligned}$$

It is straightforward to show that

$$\begin{aligned} (D.3) \quad R_i^{(2)} &= 2\omega_C^i \frac{\bar{u}_{i+1} - 2\bar{u}_i + \bar{u}_{i-1}}{(\Delta x)^2} = 2 \left(\frac{1}{2} + e_C^i \right) \left[\frac{\bar{u}_{i+1} - 2\bar{u}_i + \bar{u}_{i-1}}{(\Delta x)^2} \right] \\ &= \left(1 + \mathcal{O}((\Delta x)^2) \right) \left[\bar{u}''_i + \frac{(\Delta x)^2}{12} \bar{u}^{(4)}_i \right] = u''_i + \mathcal{O}((\Delta x)^2). \end{aligned}$$

From (D.1), (D.2) and (D.3), we confirm that (2.19) satisfies the condition (2.15) with $k = 2$.

APPENDIX E. EXPLICIT FORM OF $R_i^{(\ell)}$.

For $k = 4$ in the 1D Algorithm 2.2.3, we can take CWENO35 reconstruction as a basic reconstruction R . We refer to [6] for details on CWENO35 reconstruction. Here we can represent it as the following explicit form of $R_i(x)$:

$$(E.1) \quad R_i(x) = \sum_{\ell=0}^4 \frac{R_i^{(\ell)}}{\ell!} (x - x_i)^{(\ell)},$$

with

$$\begin{aligned}
(E.2) \quad R_i^{(0)} &= \omega_C \left(\frac{577}{480} u_i - \frac{29}{240} u_{i-1} + \frac{19}{960} u_{i-2} - \frac{29}{240} u_{i+1} + \frac{19}{960} u_{i+2} \right) \\
&\quad - \omega_2 \left(\frac{u_{i-1} - 26u_i + u_{i+1}}{24} \right) + \omega_1 \left(\frac{23}{24} u_i + \frac{1}{12} u_{i-1} - \frac{1}{24} u_{i-2} \right) + \omega_3 \left(\frac{23}{24} u_i + \frac{1}{12} u_{i+1} - \frac{1}{24} u_{i+2} \right) \\
R_i^{(1)} &= -\omega_C \frac{8u_{i-1} - u_{i-2} - 8u_{i+1} + u_{i+2}}{12\Delta x} + \omega_1 \frac{3u_i - 4u_{i-1} + u_{i-2}}{2\Delta x} \\
&\quad - \omega_3 \frac{3u_i - 4u_{i+1} + u_{i+2}}{2\Delta x} - \omega_2 \frac{u_{i-1} - u_{i+1}}{2\Delta x} \\
R_i^{(2)} &= 2 \left(\omega_1 \frac{u_i - 2u_{i-1} + u_{i-2}}{2(\Delta x)^2} + \omega_2 \frac{u_{i-1} - 2u_i + u_{i+1}}{2(\Delta x)^2} + \omega_3 \frac{u_i - 2u_{i+1} + u_{i+2}}{2(\Delta x)^2} \right) \\
&\quad - 2\omega_C \left(\frac{10u_i - 6u_{i-1} + u_{i-2} - 6u_{i+1} + u_{i+2}}{4(\Delta x)^2} \right) \\
R_i^{(3)} &= 6\omega_C \left(\frac{u_{i-1} - u_{i+1}}{3(\Delta x)^3} - \frac{u_{i-2} - u_{i+2}}{6(\Delta x)^3} \right), \quad R_i^{(4)} = 24\omega_C \left(\frac{u_{i-2} + 6u_i + u_{i+2}}{12(\Delta x)^4} - \frac{u_{i-1} + u_{i+1}}{3(\Delta x)^4} \right).
\end{aligned}$$

where the non-linear weights ω_k^i are computed as in (2.18). (See also [6].)

The CWENOZ5 reconstruction also can be directly obtained from [13] with the following non-linear weights:

$$(E.3) \quad \omega_k^i = \frac{\alpha_k^i}{\sum_\ell \alpha_\ell^i}, \quad \alpha_k^i = C_i \left(1 + \frac{\tau}{\epsilon + \beta_k^i} \right)^t, \quad k, \ell \in \{1, 2, 3, C\},$$

where $t \geq 1$ and $\tau = |\beta_3^i - \beta_1^i|$.

APPENDIX F. PROOF OF PROPOSITION 3.1

Proof. Recall the index set in (3.5). For each index set, apply corresponding approximations in (3.4) to (3.3). Then,

$$\begin{aligned}
(F.1) \quad Q_{i+\theta, j+\eta} &= \sum_{|\ell|=0}^k (\Delta)^\ell \left(\alpha_{\ell_1}(\theta) \alpha_{\ell_2}(\eta) u_{i,j}^{(\ell)} + \beta_{\ell_1}(\theta) \alpha_{\ell_2}(\eta) u_{i+1,j}^{(\ell)} \right. \\
&\quad \left. + \alpha_{\ell_1}(\theta) \beta_{\ell_2}(\eta) u_{i,j+1}^{(\ell)} + \beta_{\ell_1}(\theta) \beta_{\ell_2}(\eta) u_{i+1,j+1}^{(\ell)} \right) + \mathcal{O}(h^{k+2}).
\end{aligned}$$

Now, we consider Taylor's expansion of $u_{i+1,j}^{(\ell)}, u_{i,j+1}^{(\ell)}, u_{i+1,j+1}^{(\ell)}$:

$$\begin{aligned}
u_{i+1,j}^{(\ell)} &= \sum_{m_1=0}^{k-|\ell|} \frac{u_{i,j}^{(\ell_1+m_1, \ell_2)}}{m_1!} (\Delta x)^{m_1} + \frac{u_{i,j}^{(\ell_1+k-|\ell|+s, \ell_2)}}{(k-|\ell|+s)!} (\Delta x)^{k-|\ell|+s} \\
u_{i,j+1}^{(\ell)} &= \sum_{m_2=0}^{k-|\ell|} \frac{u_{i,j}^{(\ell_1, \ell_2+m_2)}}{m_2!} (\Delta y)^{m_2} + \frac{u_{i,j}^{(\ell_1, \ell_2+k-|\ell|+s)}}{(k-|\ell|+s)!} (\Delta x)^{k-|\ell|+s} \\
u_{i+1,j+1}^{(\ell)} &= \sum_{|m|=0}^{k-|\ell|} \frac{u_{i,j}^{(\ell+m)}}{m_1! m_2!} (\Delta)^m + \sum_{|m|=k-|\ell|+s} \frac{u_{i,j}^{(\ell+m)}}{m_1! m_2!} (\Delta)^m,
\end{aligned}$$

where $m = (m_1, m_2)$ is an multi index. Inserting this into (F.1), we obtain

$$(F.2) \quad Q_{i+\theta, j+\eta} =: \sum_{|\ell|=0}^k (\Delta)^\ell \Lambda_\ell(\theta, \eta) u_{i,j}^{(\ell)} + \Gamma(\theta, \eta) + \mathcal{O}(h^{k+2}),$$

where $\Lambda_\ell(\theta, \eta)$ and $\Gamma(\theta, \eta)$ are given by

$$\begin{aligned}\Lambda_\ell(\theta, \eta) &= \alpha_{\ell_1}(\theta)\alpha_{\ell_2}(\eta) + \alpha_{\ell_2}(\eta) \sum_{m_1=0}^{\ell_1} \beta_{m_1}(\theta) \frac{1}{(\ell_1 - m_1)!} \\ &\quad + \alpha_{\ell_1}(\theta) \sum_{m_2=0}^{\ell_2} \beta_{m_2}(\eta) \frac{1}{(\ell_2 - m_2)!} + \sum_{|m|=0}^{|\ell|} \beta_{m_1}(\theta)\beta_{m_2}(\eta) \frac{1}{(\ell_1 - m_1)!(\ell_2 - m_2)!} \\ \Gamma(\theta, \eta) &= \sum_{|\ell|=0}^k \beta_{\ell_1}(\theta)\alpha_{\ell_2}(\eta) \frac{u_{i,j}^{(\ell_1+k-|\ell|+s, \ell_2)}}{(k-|\ell|+s)!} (\Delta x)^{k-|\ell|+s} (\Delta)^\ell \\ &\quad + \sum_{|\ell|=0}^k \alpha_{\ell_1}(\theta)\beta_{\ell_2}(\eta) \frac{u_{i,j}^{(\ell_1, \ell_2+k-|\ell|+s)}}{(k-|\ell|+s)!} (\Delta y)^{k-|\ell|+s} (\Delta)^\ell \\ &\quad + \sum_{|\ell|=0}^k \beta_{\ell_1}(\theta)\beta_{\ell_2}(\eta) \sum_{|m|=k-|\ell|+s} \frac{u_{i,j}^{(\ell+m)}}{m_1!m_2!} (\Delta)^{m+\ell}.\end{aligned}$$

Now, we add 0 to $\Gamma(\theta, \eta)$ using the following identity:

$$\begin{aligned}0 &= \sum_{|\ell|=k+1} (\alpha_{\ell_1}(\theta) + \beta_{\ell_1}(\theta)) (\alpha_{\ell_2}(\eta) + \beta_{\ell_2}(\eta)) u_{i,j}^{(\ell)} (\Delta)^\ell \\ (F.3) \quad &= \sum_{|\ell|=k+1} \alpha_{\ell_1}(\theta)\alpha_{\ell_2}(\eta) u_{i,j}^{(\ell)} (\Delta)^\ell + \sum_{|\ell|=k+1} \beta_{\ell_1}(\theta)\alpha_{\ell_2}(\eta) u_{i,j}^{(\ell)} (\Delta)^\ell \\ &\quad + \sum_{|\ell|=k+1} \alpha_{\ell_1}(\theta)\beta_{\ell_2}(\eta) u_{i,j}^{(\ell)} (\Delta)^\ell + \sum_{|\ell|=k+1} \beta_{\ell_1}(\theta)\beta_{\ell_2}(\eta) u_{i,j}^{(\ell)} (\Delta)^\ell,\end{aligned}$$

then

$$\begin{aligned}\Gamma(\theta, \eta) + 0 &= \sum_{|\ell|=k+1} \alpha_{\ell_1}(\theta)\alpha_{\ell_2}(\eta) u_{i,j}^{(\ell)} (\Delta)^\ell + \sum_{|\ell|=0}^{k+1} \beta_{\ell_1}(\theta)\alpha_{\ell_2}(\eta) \frac{u_{i,j}^{(\ell_1+k-|\ell|+s, \ell_2)}}{(k-|\ell|+s)!} (\Delta x)^{k-|\ell|+s} (\Delta)^\ell \\ &\quad + \sum_{|\ell|=0}^{k+1} \alpha_{\ell_1}(\theta)\beta_{\ell_2}(\eta) \frac{u_{i,j}^{(\ell_1, \ell_2+k-|\ell|+s)}}{(k-|\ell|+s)!} (\Delta y)^{k-|\ell|+s} (\Delta)^\ell \\ &\quad + \sum_{|\ell|=0}^{k+1} \beta_{\ell_1}(\theta)\beta_{\ell_2}(\eta) \sum_{|m|=k-|\ell|+s} \frac{u_{i,j}^{(\ell+m)}}{m_1!m_2!} (\Delta)^{m+\ell}.\end{aligned}$$

This reduces to

$$\Gamma(\theta, \eta) = \sum_{|\ell|=k+1} (\Delta)^\ell \Lambda_\ell(\theta, \eta) u_{i,j}^{(\ell)}.$$

Based on this formula, we rearrange all terms in (F.2) as follows:

$$\begin{aligned}
Q_{i+\theta,j+\eta} &= u_{i,j} + \theta \Delta x u'_{i,j} + \eta \Delta y u''_{i,j} + \left(\frac{\theta^2}{2} + \frac{1}{24} \right) (\Delta x)^2 u'''_{i,j} + \left(\frac{\eta^2}{2} + \frac{1}{24} \right) (\Delta y)^2 u''''_{i,j} + \eta \theta \Delta x \Delta y u''''_{i,j} \\
&\quad + \left(\frac{\theta^3}{6} + \frac{\theta}{24} \right) (\Delta x)^3 u''''''_{i,j} + \left(\frac{\eta \theta^2}{2} + \frac{\eta}{24} \right) (\Delta x)^2 \Delta y u''''''_{i,j} \\
&\quad + \left(\frac{\theta \eta^2}{2} + \frac{\theta}{24} \right) \Delta x (\Delta y)^2 u''''''_{i,j} + \left(\frac{\eta^3}{6} + \frac{\eta}{24} \right) (\Delta y)^3 u''''''''_{i,j} + \dots + \mathcal{O}(h^{k+2}) \\
&= u_{i+\theta,j+\eta} + \frac{(\Delta x)^2}{24} u''_{i+\theta,j+\eta} + \frac{(\Delta y)^2}{24} u''''_{i+\theta,j+\eta} + \dots + \mathcal{O}(h^{k+2}) \\
&= \bar{u}_{i+\theta,j+\eta} + \mathcal{O}(h^{k+2}),
\end{aligned}$$

which completes the proof. \square

APPENDIX G. SEMI-LAGRANGIAN SCHEMES FOR HYPERBOLIC SYSTEM WITH BDF METHODS

The BDF methods [20] for an ordinary system $y'(t) = f(y)$ can be represented by

$$y^{n+1} = \sum_{k=1}^s \alpha_k y^{n+1-s} + \beta_s f^{n+1}.$$

where α_k and β_s are coefficients corresponding to s-order BDF methods. Here, we consider two cases $s = 2, 3$:

$$\begin{aligned}
\text{BDF2: } y^{n+1} &= \frac{4}{3} y^n - \frac{1}{3} y^{n-1} + \frac{2}{3} f^{n+1} \\
\text{BDF3: } y^{n+1} &= \frac{18}{11} y^n - \frac{9}{11} y^{n-1} + \frac{2}{11} y^{n-2} + \frac{6}{11} f^{n+1}.
\end{aligned}$$

G.1. BDF methods for Xin-Jin model. Applying BDF method based SL methods to (4.7), we obtain:

$$\begin{aligned}
(G.1) \quad f_i^{n+1} &= \sum_{k=1}^s \alpha_k \tilde{f}^{n,k} + \beta_s \frac{\Delta t}{\kappa} K_{i,1}^{n+1} \\
g_i^{n+1} &= \sum_{k=1}^s \alpha_k \tilde{g}^{n,k} + \beta_s \frac{\Delta t}{\kappa} K_{i,2}^{n+1}.
\end{aligned}$$

Here we use the following notation:

- For $k = 1, \dots, s$, the $(n+1-k)$ th stage values of f, g along the backward-characteristics which come from x_i with characteristic speed $-1, 1$ at time t^{n+1} :

$$\tilde{f}_i^{n,k} \approx f(x_i + k\Delta t, t^{n+1-k}), \quad \tilde{g}_i^{n,k} \approx g(x_i - k\Delta t, t^{n+1-k}).$$

- Fluxes at time t^{n+1} :

$$K_{i,1}^{n+1} \approx F(u_i^{n+1}) - v_i^{n+1}, \quad K_{i,2}^{n+1} \approx -K_{i,1}^{n+1}.$$

The algorithm can be summarized as follows:

Algorithm of s-order BDF methods.

- (1) For $k = 1, 2, \dots, s$, interpolate $\tilde{f}_i^{n,k}$ and $\tilde{g}_i^{n,k}$ on $x_i + k\Delta t$ and $x_i - k\Delta t$ from $\{f_i^{n+1-k}\}$ and $\{g_i^{n+1-k}\}$, respectively.

(2) By summing and subtracting two equations in (G.1), compute:

$$\begin{aligned} u_i^{n+1} &= \frac{\sum_{k=1}^s \alpha_k (\tilde{g}_i^{n,k} + \tilde{f}_i^{n,k})}{2} \\ v_i^{n+1} &= \frac{\kappa \sum_{k=1}^s \alpha_k (\tilde{g}_i^{n,k} - \tilde{f}_i^{n,k}) / 2 + \beta_k \Delta t F(u_i^{n+1})}{\kappa + \beta_s \Delta t}. \end{aligned}$$

(3) Compute:

$$f_i^{n+1} = u_i^{n+1} - v_i^{n+1}, \quad g_i^{n+1} = u_i^{n+1} + v_i^{n+1}$$

G.2. BDF methods for Broadwell model. Now, we extend this to high order s-order BDF methods. The solutions are obtained by

$$\begin{aligned} f_i^{n+1} &= \sum_{\ell=1}^s \alpha_k f_i^{n,k} + \frac{\beta_s \Delta t}{\kappa} Q_i^{n+1} \\ g_i^{n+1} &= \sum_{\ell=1}^s \alpha_k g_i^{n,k} + \frac{\beta_s \Delta t}{\kappa} Q_i^{n+1} \\ h_i^{n+1} &= \sum_{\ell=1}^s \alpha_k h_i^{n+1-k} - \frac{\beta_s \Delta t}{\kappa} Q_i^{n+1} \end{aligned} \tag{G.2}$$

where

$$Q_i^{n+1} = (h_i^{n+1})^2 - f_i^{n+1} g_i^{n+1}, \quad f_i^{n,k} \approx f(x_i - k \Delta t, t^{n+1-k}), \quad g_i^{n,k} \approx g(x_i + k \Delta t, t^{n+1-k}),$$

Then, s-order BDF methods are summarized as follows:

Algorithm of s-order BDF methods.

- (1) Reconstruct $f_i^{n,k}$ and $g_i^{n,k}$ for $k = 1, \dots, s$.
- (2) Compute F_i^n , G_i^n and H_i^n using

$$F_i^n := \sum_{\ell=1}^s \alpha_k f_i^{n,k}, \quad G_i^n := \sum_{\ell=1}^s \alpha_k g_i^{n,k}, \quad H_i^n := \sum_{\ell=1}^s \alpha_k h_i^{n+1-k}.$$

- (3) Solve (G.2) for

$$\begin{aligned} h_i^{n+1} &= \frac{\beta_s \Delta t (H_i^n + F_i^n)(H_i^n + G_i^n) + \kappa H_i^n}{\beta_s \Delta t (G_i^n + 2H_i^n + F_i^n) + \kappa}, \\ f_i^{n+1} &= H_i^n + F_i^n - h_i^{n+1}, \quad g_i^{n+1} = H_i^n + G_i^n - h_i^{n+1}. \end{aligned}$$

ACKNOWLEDGMENTS

S. Y. Cho has been supported by ITN-ETN Horizon 2020 Project ModCompShock, Modeling and Computation on Shocks and Interfaces, Project Reference 642768. S.-B. Yun has been supported by Samsung Science and Technology Foundation under Project Number SSTF-BA1801-02. All the authors would like to thank the Italian Ministry of Instruction, University and Research (MIUR) to support this research with funds coming from PRIN Project 2017 (No. 2017KKJP4X entitled Innovative numerical methods for evolutionary partial differential equations and applications). S. Boscarino has been supported by the University of Catania (Piano della Ricerca 2016/2018, Linea di intervento 2). S. Boscarino and G. Russo are members of the INdAM Research group GNCS.

REFERENCES

1. S. Boscarino, S.-Y. Cho, G. Russo, and S.-B. Yun, *High order conservative semi-lagrangian scheme for the bgk model of the boltzmann equation*, arXiv preprint arXiv:1905.03660 (2019).
2. S. Boscarino and G. Russo, *On a class of uniformly accurate imex runge–kutta schemes and applications to hyperbolic systems with relaxation*, SIAM Journal on Scientific Computing **31** (2009), no. 3, 1926–1945.
3. J. E. Broadwell, *Shock structure in a simple discrete velocity gas*, The Physics of Fluids **7** (1964), no. 8, 1243–1247.
4. R. E. Caflisch, S. Jin, and G. Russo, *Uniformly Accurate Schemes for Hyperbolic Systems with Relaxation*, SIAM J. Numer. Anal. **34** (1997), no. 1, 246–281.
5. M. Campos-Pinto, F. Charles, and B. Després, *Algorithms for positive polynomial approximation*, SIAM Journal on Numerical Analysis **57** (2019), no. 1, 148–172.
6. G. Capdeville, *A central WENO scheme for solving hyperbolic conservation laws on non-uniform meshes*, J. Comput. Phys. **227** (2008), no. 5, 2977–3014.
7. E. Carlini, R. Ferretti, and G. Russo, *A Weighted Essentially Nonoscillatory, Large Time-Step Scheme for Hamilton–Jacobi Equations*, SIAM J. Sci. Comput. **27** (2005), no. 3, 1071–1091.
8. J. A. Carrillo and F. Vecil, *Nonoscillatory interpolation methods applied to vlasov-based models*, SIAM Journal on Scientific Computing **29** (2007), no. 3, 1179–1206.
9. M. Castro, B. Costa, and W. S. Don, *High order weighted essentially non-oscillatory WENO-Z schemes for hyperbolic conservation laws*, J. Comput. Phys. **230** (2011), 1766–1792.
10. C. Cercignani, *The Boltzmann Equation and Its Applications*, Springer, New York, 1988.
11. G. Q. Chen, C. D. Levermore, and T. P. Liu, *Hyperbolic conservation laws with stiff relaxation terms and entropy*, Communications on Pure and Applied Mathematics **47** (1994), no. 6, 787–830.
12. I. Cravero, G. Puppo, M. Semplice, and G. Visconti, *CWENO: uniformly accurate reconstructions for balance laws*, Math. Comp. **87** (2017), no. 312, 1689–1719.
13. ———, *Cool WENO schemes*, Computers and Fluids **169** (2018), 71–86.
14. N. Crouseilles, M. Mehrenberger, and E. Sonnendrcker, *Conservative semi-Lagrangian schemes for Vlasov equations*, J. Comput. Phys. **229** (2010), no. 6, 1927–1953.
15. M. Dehghan and M. Abbaszadeh, *The space-splitting idea combined with local radial basis function meshless approach to simulate conservation laws equations*, Alexandria Engineering Journal **57** (2018), no. 2, 1137–1156.
16. M. Dumbser, W. Boscheri, M. Semplice, and G. Russo, *Central weighted eno schemes for hyperbolic conservation laws on fixed and moving unstructured meshes*, SIAM Journal on Scientific Computing **39** (2017), no. 6, A2564–A2591.
17. F. Filbet and E. Sonnendrücker, *Comparison of eulerian vlasov solvers*, Comput. Phys. Commun. **150** (2001), no. IRMA-2001-035, 247–266.
18. F. Filbet, E. Sonnendrücker, and P. Bertrand, *Conservative numerical schemes for the vlasov equation*, J. Comput. Phys. **172** (2001), 166–187.
19. J. Friedrich and O. Kolb, *Maximum principle satisfying cweno schemes for nonlocal conservation laws*, SIAM J. Sci. Comput. **41** (2019), no. 2, A973–A988.
20. E. Hairer and G. Warner, *Solving Ordinary Differential Equations II: Stiff and Differential-Algebraic Problems*, Springer, Berlin, 1996.
21. E. Hairer, G. Warner, and S. P. Nørsett, *Solving Ordinary Differential Equations I: Nonstiff Problem*, Springer, Berlin, 1996.
22. S. Jin, *Asymptotic preserving (AP) schemes for multiscale kinetic and hyperbolic equations: A review*, Lecture Notes for Summer School on "Methods and Models of Kinetic Theory" (M&MKT), Porto Ercole (Grosseto, Italy), Riv. Math. Univ. Parma **3** (2010), 177–216.
23. S. Jin and C. D. Levermore, *Numerical schemes for hyperbolic conservation laws with stiff relaxation terms*, J. Comput. Phys. **126** (1996), no. 2, 449–467.
24. S. Jin and Z. Xin, *The relaxation schemes for systems of conservation laws in arbitrary space dimensions*, Communications on pure and applied mathematics **48** (1995), no. 3, 235–276.
25. C. Kennedy and M. H. Carpenter, *Additive RungeKutta schemes for convectiondiffusionreaction equations*, Applied Numerical Mathematics **44** (2003), no. 1-2, 139–181.
26. O. Kolb, *On the full and global accuracy of a compact third order weno scheme*, SIAM J. Numer. Anal. **52** (2014), no. 5, 2335–2355.
27. D. Levy, G. Puppo, and G. Russo, *Central WENO schemes for hyperbolic systems of conservation laws*, ESAIM: Mathematical Modelling and Numerical Analysis **33** (1999), no. 3, 547–571.
28. ———, *Compact central WENO schemes for multidimensional conservation laws*, SIAM J. Sci. Comput. **22** (2000), no. 2, 656–672.
29. ———, *A fourth order central weno scheme for multidimensional hyperbolic systems of conservation laws*, SIAM J. Sci. Comput. **24** (2002), no. 2, 480–506.
30. Y. Y. Liu, C. W. Shu, and M. P. Zhang, *On the positivity of linear weights in WENO approximations*, Acta Mathematicae Applicatae Sinica **25** (2009), no. 3, 503–538.

31. L. Pareschi and G. Russo, *Implicit-explicit runge-kutta schemes and applications to hyperbolic systems with relaxation*, J. Sci. Comput. **25** (2005), no. 1, 129–155.
32. J. M. Qiu and C. W. Shu, *Conservative Semi-Lagrangian Finite Difference WENO Formulations with Applications to the Vlasov Equation*, Communications in Computational Physics **10** (2011), no. 4, 979–1000.
33. G. Russo, J. Qiu, and X. Tao, *Conservative Multi-Dimensional Semi-Lagrangian Finite Difference Scheme: Stability and Applications to the Kinetic and Fluid Simulations*, J. Sci. Comput. (2018), 1–30.
34. J. W. Schmidt and W. Hess, *Positivity of cubic polynomials on intervals and positive spline interpolation*, BIT Numerical Mathematics **28** (1988), no. 2, 340–352.
35. C. W. Shu, *Essentially non-oscillatory and weighted essentially non-oscillatory schemes for hyperbolic conservation laws*, Advanced numerical approximation of nonlinear hyperbolic equations, Springer, 1998, pp. 325–432.
36. G. B. Whitham, *Linear and nonlinear waves*, John Wiley and Sons, New York, 1974.
37. X. Zhang and C.-W. Shu, *On maximum-principle-satisfying high order schemes for scalar conservation laws*, Journal of Computational Physics **229** (2010), no. 9, 3091–3120.
38. ———, *Maximum-principle-satisfying and positivity-preserving high-order schemes for conservation laws: survey and new developments*, Proceedings of the Royal Society A: Mathematical, Physical and Engineering Sciences **467** (2011), no. 2134, 2752–2776.

SEUNG YEON CHO, DEPARTMENT OF MATHEMATICS AND COMPUTER SCIENCE, UNIVERSITY OF CATANIA, 95125 CATA-NIA, ITALY

E-mail address: chosy89@skku.edu

SEBASTIANO BOSCARINO, DEPARTMENT OF MATHEMATICS AND COMPUTER SCIENCE, UNIVERSITY OF CATANIA, 95125 CATANIA, ITALY

E-mail address: boscarino@dmi.unict.it

GIOVANNI RUSSO, DEPARTMENT OF MATHEMATICS AND COMPUTER SCIENCE, UNIVERSITY OF CATANIA, 95125 CATA-NIA, ITALY

E-mail address: russo@dmi.unict.it

SEOK-BAE YUN, DEPARTMENT OF MATHEMATICS, SUNGKYUNKWAN UNIVERSITY, SUWON 440-746, REPUBLIC OF KOREA

E-mail address: sbyun01@skku.edu